



## ORIGINAL ARTICLE

# Pharmacokinetics under the COVID-19 storm

Venkatesh Pilla Reddy<sup>1,2</sup>  | Eman El-Khateeb<sup>3,4</sup>  | Heeseung Jo<sup>1</sup> |  
 Natalie Giovino<sup>5</sup> | Emily Lythgoe<sup>6</sup> | Shringi Sharma<sup>7</sup> | Weifeng Tang<sup>7</sup> |  
 Masoud Jamei<sup>8</sup> | Amin Rastomi-Hodjegan<sup>3,8</sup>

<sup>1</sup>Modelling & Simulation, Early Oncology, R&D Oncology, AstraZeneca, Cambridge, UK

<sup>2</sup>Clinical Pharmacology and Quantitative Pharmacology, R&D, AstraZeneca, Cambridge, UK

<sup>3</sup>Centre for Applied Pharmacokinetic Research, University of Manchester, Manchester, UK

<sup>4</sup>Clinical Pharmacy Department, Faculty of Pharmacy, Tanta University, Tanta, Egypt

<sup>5</sup>Early Oncology Clinical, R&D Oncology, AstraZeneca, Boston, USA

<sup>6</sup>R&D Biopharmaceuticals, AstraZeneca, Cambridge, UK

<sup>7</sup>Clinical Pharmacology and Quantitative Pharmacology, R&D, AstraZeneca, USA

<sup>8</sup>Certara UK Limited, Simcyp Division, Sheffield, UK

## Correspondence

Dr Venkatesh Pilla Reddy, Clinical Pharmacology and Quantitative Pharmacology, R&D, AstraZeneca, Aaron Klug Building, Granta Park, Cambridge CB21 6GH, UK.  
 Email: venkatesh.reddy@astrazeneca.com

**Aims:** The storm-like nature of the health crises caused by COVID-19 has led to unconventional clinical trial practices such as the relaxation of exclusion criteria. The question remains: how can we conduct diverse trials without exposing subgroups of populations to potentially harmful drug exposure levels? The aim of this study was to build a knowledge base of the effect of intrinsic/extrinsic factors on the disposition of several repurposed COVID-19 drugs.

**Methods:** Physiologically based pharmacokinetic (PBPK) models were used to study the change in the pharmacokinetics (PK) of drugs repurposed for COVID-19 in geriatric patients, different race groups, organ impairment and drug-drug interactions (DDIs) risks. These models were also used to predict epithelial lining fluid (ELF) exposure, which is relevant for COVID-19 patients under elevated cytokine levels.

**Results:** The simulated PK profiles suggest no dose adjustments are required based on age and race for COVID-19 drugs, but dose adjustments may be warranted for COVID-19 patients also exhibiting hepatic/renal impairment. PBPK model simulations suggest ELF exposure to attain a target concentration was adequate for most drugs, except for hydroxychloroquine, azithromycin, atazanavir and lopinavir/ritonavir.

**Conclusion:** We demonstrate that systematically collated data on absorption, distribution, metabolism and excretion, human PK parameters, DDIs and organ impairment can be used to verify simulated plasma and lung tissue exposure for drugs repurposed for COVID-19, justifying broader patient recruitment criteria. In addition, the PBPK model developed was used to study the effect of age and ethnicity on the PK of repurposed drugs, and to assess the correlation between lung exposure and relevant potency values from in vitro studies for SARS-CoV-2.

## KEYWORDS

ADME, COVID-19, cytokine, Drug-Drug Interactions, M&S, PBPK, PKPD

## 1 | INTRODUCTION

### 1.1 | “Necessity is the mother of invention”

Desperate times have often led to unorthodox approaches to address an unmet need. Clinical trials in drug development are not an exception to this. In general, clinical trials are conducted in a systematic way and

follow stringent recruitment criteria. Lack of diversity in patients recruited to drug trials was the subject of a recent draft Guidance for Industry by the US Food and Drug Administration (FDA), where they encouraged inclusion of the elderly, those at the extremes of the weight range, individuals with organ dysfunction, those with malignancies or certain infections such as HIV, and children.<sup>1</sup> This guidance emphasized the need to characterize drugs more comprehensively during early

clinical development (eg, with respect to drug metabolism and clearance pathways). In addition, the guidance indicated that dose adjustments can be made in specific populations to reduce significant differences in systemic exposure to the drug under investigation. However, broadened recruitment of patients in COVID-19 drug trials has been an exception to the norm resulting from the speed of transmission of the virus (the reproduction rate is 2.65 days). The pandemic has accelerated the adoption of the draft guidance on broadening recruitment. However, this risks exposing subgroups of populations to higher drug levels, particularly for drugs that lack safety studies specific to these subgroups.

## 1.2 | COVID-19 pandemic in perspective

Several therapeutic agents have been evaluated for the treatment of COVID-19, but remdesivir, acalabrutinib, ibrutinib and dexamethasone in particular have shown some positive results.<sup>2-4</sup> The FDA has issued guidance for COVID-19 trials<sup>5</sup> emphasizing the need to consider participant safety alongside the need to establish the efficacy of drugs against SARS-CoV-2. The estimated basic reproduction rate for SARS-CoV-2 is 2.65 days (with a range from 1.85 to 3.41 days).<sup>6</sup>

## 1.3 | Drugs on trial for COVID-19

As of 21 May 2020 there were 1621 COVID-19 trials on [clinicaltrials.gov](https://clinicaltrials.gov), of which 912 are active and/or recruiting. To address the urgent need for therapeutic remedies for COVID-19, efforts to repurpose existing drugs are increasing, hence most trials are focused on existing drugs rather than investigating new drugs. These repurposed drugs consist of antivirals (azithromycin, atazanavir, baloxavir, darunavir, lopinavir, remdesivir, ritonavir), anticancer drugs (acalabrutinib, ibrutinib, baricitinib, ruxolitinib), anti-inflammatories (dexamethasone), large molecules (siltuximab, emapalumab, tocilizumab), antimalarials (chloroquine, hydroxychloroquine), and one antidiabetic and heart failure treatment drug (dapagliflozin). Azithromycin is dosed in combination with hydroxychloroquine.<sup>7</sup>

## 1.4 | Typical COVID-19 patient and cytokine storm

A typical hospitalized COVID-19 patient exhibits overproduction of early response pro-inflammatory cytokines such as tumour necrosis factor (TNF), interleukin-6 (IL-6) and interleukin-1 beta (IL-1 $\beta$ ). This is known as a “cytokine storm” and is thought to be one of the major causes of acute respiratory distress syndrome (ARDS) and multiple-organ failure.<sup>8</sup> Patients presenting with cytokine release syndrome typically show cytopenia, elevated creatinine, deranged coagulation parameters and high C-reactive protein (CRP).<sup>9</sup> The common symptoms and cascade of a COVID-19-induced cytokine storm<sup>10</sup> are depicted in Figure 1. Due to the relationship between cytokine release syndrome and poor outcomes among COVID-19 patients, many of the drugs (small

### What is already known about this subject

- Disease-drug interactions can result in exposure changes, which are well documented in cancer, cirrhosis and rheumatoid arthritis. Cytokine storms are known to perturb the expression of cytochrome P450 enzymes, conjugative enzymes and transporters.
- Clinically observed pharmacokinetic data and knowledge of the effects of race on repurposed COVID-19 drugs in geriatric COVID-19 patients are limited.
- There is some knowledge of the effect of intrinsic and extrinsic factors on the disposition of repurposed COVID-19 drugs, but dosing recommendations for patients with a cytokine storm are lacking.

### What this study adds

- A comprehensive summary of absorption, distribution, metabolism and excretion, DDIs, adverse events and simulated lung exposure for COVID-19 repurposed drugs.
- Verified physiologically based pharmacokinetic models that predict changes in drug exposure in various clinical scenarios, guiding dosing information where it is not possible to obtain clinical data, particularly given the COVID-19 pandemic
- Simulated plasma and lung tissue exposure of drugs to justify broader recruitment criteria for patients and assess the relevant potency values from in vitro studies for SARS-CoV-2.

molecules and biologicals) currently being tested aim to dampen this severe immune response, while others target the virus' ability to infect cells. Inflammation resulting from cytokine release starts locally, in areas such as pulmonary tissue, and spreads to other organs through systemic circulation. This triggers compensatory biological repair processes which restore tissue and organ function; however, these processes can lead to fibrosis and persistent organ dysfunction of the lungs, heart, liver and kidney.<sup>11</sup> Many small molecule drugs are metabolized by cytochrome P450 (CYP450) enzymes typically expressed in the liver, gut, lung and kidney. Several pro-inflammatory cytokines (IL-1 $\beta$ , IL-6, TNF- $\alpha$ ) have been reported to downregulate the expression of these enzymes and transporters such as P-glycoprotein (P-gp) by inducing transcription factors (eg, Pregnane X receptor (PXR), Chimeric antigen receptor (CAR), Nuclear factor (NF- $\kappa$ B), and Hepatocyte nuclear factor (HNF)), which in turn reduce the abundance of CYP450 and P-gp in tissues.<sup>12</sup> This influences the absorption, distribution and metabolism of drugs, as represented in Figure 1.

Elevated cytokine levels alter the pharmacokinetics (PK), and thus exposure, of small molecules. A few clinical studies have compared drug exposure before and after treatment with cytokines. The use of

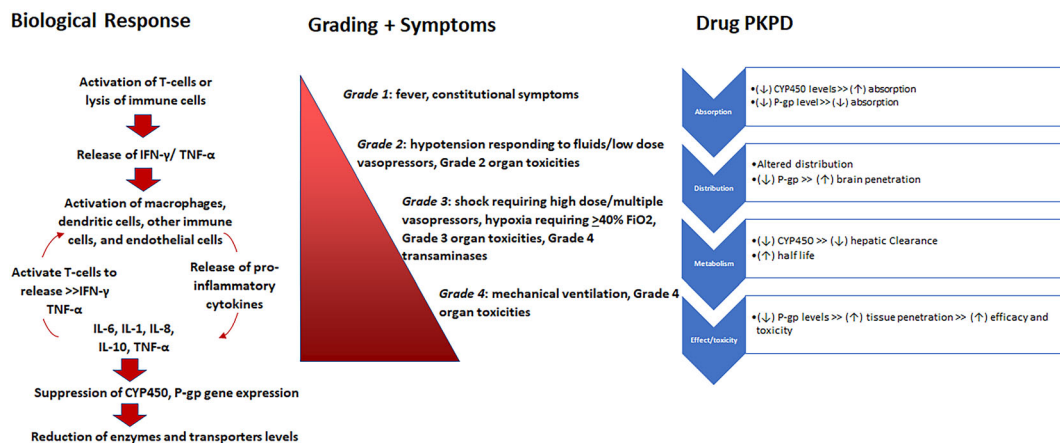


**FIGURE 1** Symptoms and grades of cytokine release syndrome, also known as cytokine storm, and its impact on drug exposure

interferon (IFN)- $\alpha$  in chronic hepatitis B has been found to decrease theophylline (metabolized mainly by CYP1A2) clearance by 50% and prolong the half-life of the drug by 70%.<sup>13</sup> Alternatively, blocking IL-6 receptor activity with drugs such as sarilumab and tocilizumab reduces the AUC and  $C_{max}$  of simvastatin (CYP3A4 substrate) by 40-57%.<sup>14,15</sup>

As clinical studies addressing the impact of different drug metabolizing enzymes and transporters are not always feasible, in vitro models of hepatic and intestinal cell lines can be used. Exposure of Hepatoma cell line (hepaRG) hepatic cells to IL-6 (10 ng/mL) for 72 hours has been found to decrease CYP3A4 mRNA expression and activity by more than 80%, CYP1A2 activity by 60%, and CYP2B6 and 2C19 activity by 80%.<sup>16</sup> In epiintestinal cells the expression of phase I enzymes CYP2C19, CYP2C9 and CYP3A4 was reduced by 40-50% (Monoamine oxidase A [MAO A] 35%, Monoamine oxidase B [MAO B] 42%), whilst activities of CYP2C19, CYP2C9 and CYP3A4 were suppressed by 20-75% following exposure to IL-6. However, it is worth noting that extrapolation of in vitro results to in vivo models is challenging due to the complexity of biological systems, disease pathophysiology, degrees of severity, changes in cytokines levels and interactions among cytokines and DME targets.<sup>17</sup> One added difficulty, for example, is making sure that IL-6 is added to cells in concentrations that mimic physiological levels in healthy and diseased states.<sup>18</sup>

## 1.5 | Information on study subpopulations

Remdesivir clinical trial<sup>2</sup> patient characteristics included chronic liver (2%) and kidney disease (6%), cancer (8%) and obesity (37%). Thirty-six per cent of patients were  $>65$  years and patients of different race were included in the trial population. A large proportion of COVID-19 patients requiring hospitalization and treatment are geriatric<sup>19</sup> and it is likely that this patient population may exhibit exposure differences. The possibility of testing the effect of intrinsic and extrinsic factors clinically is limited, for instance PK on geriatric COVID-19 patients.

## 1.6 | Physiologically based pharmacokinetic models

The pharmacokinetic, absorption, distribution, metabolism and excretion (ADME) data for single or multiple doses is relatively abundant for COVID-19 repurposed drugs and can be used to build physiologically based pharmacokinetic (PBPK) models. These models utilize three components: a system component, a drug-dependent component and a clinical trial-specific component. Details of human physiology are specified in system components, for instance drug metabolizing enzyme or transporter abundance, tissue blood flow to organs and so on. Drug properties such as solubility, fraction metabolized by enzymes and renal clearance are specified in the drug-dependent components, whilst the clinical trial-specific component defines the simulated scenario, including dosing regimen, population age and gender proportion. PBPK models combine these components to predict drug ADME, and by extension PK, in a simulated scenario where clinical study data are not available. These verified PBPK models can provide the ability to extrapolate beyond the available data and account for disease-drug interactions.<sup>20,21</sup>

## 1.7 | Target site concentrations

As COVID-19 mainly targets lung tissue, making it difficult to assess tissue concentration, understanding expected target concentration may be crucial, particularly when attempting to translate observed effect from the in vitro studies to projected clinical situations. PBPK models are useful to predict drug unbound concentrations in the epithelial lining fluid (ELF),<sup>22</sup> which is relevant for treatment of COVID-19 patients as it can contain a persistent reservoir of the virus.

The objectives of this study were to gather information on the ADME, PK/pharmacodynamic (PK/PD), drug-drug interactions

(DDIs), adverse events (AEs), and the effect of intrinsic and extrinsic factors on the disposition of all repurposed drugs currently under trial for COVID-19. This enabled us to explore the utility of PBPK models for possible clinical scenarios after verifying them based on the gathered preclinical and clinical data. Then we used the models to predict expected alterations in exposure to these drugs in sub-populations of COVID-19 patients which have not yet been studied for some of the drugs, eg, in patients with older age, different race and hepatic/renal impairment. These variations were studied in relation to target site concentrations.

## 2 | METHODS

### 2.1 | Clinical PK and PD data extraction of COVID-19 repurposed compounds and COVID-19 patient characteristics

Trials of drugs repurposed for COVID-19 were selected in this work from the American Society of Health-System Pharmacists (ASHP) list.<sup>23</sup> In addition, two drugs from AstraZeneca currently being studied in clinical trials were included, acalabrutinib, a Bruton tyrosine kinase (BTK) inhibitor,<sup>3</sup> and dapagliflozin, a sodium-glucose transport protein 2 (SGLT2) inhibitor. Details of these and other repurposed drugs are summarized in detail in Table 1 and in the **Supporting Information** text. These repurposed drugs were antivirals (azithromycin, atazanavir, baloxavir, darunavir, lopinavir, remdesivir, ritonavir), anticancer drugs (acalabrutinib, baricitinib, ruxolitinib), anti-inflammatories and immunomodulators (dexamethasone), biologicals (siltuximab, emapalumab, tocilizumab), antimalarials (chloroquine, hydroxychloroquine), and antidiabetic and heart failure treatment drugs (dapagliflozin). Clinical studies for probe compounds were queried with appropriate literature searches and through the University of Washington Drug Interaction Database (UWDIDB). Dosing regimens, relevant PK parameters, DDIs, AEs and applicable demographic data, such as age, gender, race, PK in hepatic and renal impairment, and genotype, were manually extracted from the selected publications. Cytokine information, such as IL-6 levels in a typical COVID-19 patient, was extracted from literature and compared with other cytokine storm disease conditions such as cancer, rheumatoid arthritis and cirrhosis etc.

**TABLE 1** Interleukin-6 (IL-6) levels reported in different diseases, including COVID-19

IL-6 levels	pg/mL	Number of cases	Reference
Healthy	1.3-10.3	312	<sup>24</sup>
Cirrhosis	18-146	63	<sup>25</sup>
RA	18-109	40	<sup>26</sup>
Cancer	0.23-78.5	1272 (from 72 studies)	<sup>27</sup>
COVID-19	21 (mild)-66 (severe)	17	<sup>8</sup>

### 2.2 | PBPK model development to study the effect of age, race and organ dysfunction

PBPK modelling and simulations were performed using a Simcyp V19 simulator (Certara UK Ltd, Sheffield, UK) for clinical trial scenarios as shown in **Supporting Information Figure S1**. Well-established or fit-for-purpose PBPK models were verified against available clinical data before being utilized to simulate scenarios where no clinical data are available. PBPK models of acalabrutinib, baricitinib, ruxolitinib, ritonavir, darunavir and dapagliflozin were previously verified extensively and have been submitted previously as part of new drug application submission to the FDA. The rest of the PBPK models (azithromycin, atazanavir, lopinavir, chloroquine, hydroxychloroquine) were reported in peer-reviewed journals with a reasonable level of verification. These verified PBPK compound files were obtained from either Simcyp Simulator compound library files or repository files (<https://members.simcyp.com/account/libraryFiles/>) or were built using reported compound input parameters. The PBPK model input parameters are shown in **Supporting Information Table S1** and the key drug parameters required for simulating lung concentration are shown in **Supporting Information Table S2**. Trial designs for all simulations were set to 10 trials of 10 patients with the relevant populations constrained by age range and the proportion of females which reflected the reported study design of clinical studies where available. Dosing amounts and schedules were chosen as per the respective compound dosing recommendations and administered as an oral single dose or multiple dose across all simulations. Darunavir and lopinavir simulations were run as combination therapies with ritonavir as a booster drug. The predictive performance PBPK model of probe compounds was measured by the ratio of the mean predicted AUC to the mean observed AUC where possible (**Supporting Information Table S3**). For organ dysfunction simulations,  $AUC_{\text{diseased}}$  to  $AUC_{\text{healthy}}$  ratios for both observed and predicted scenarios were calculated as predictive performance measures. The predictability was considered acceptable if this metric fell between the upper and lower limits (0.5- to 2-fold of observed data). Differences in exposure from race in Caucasian, Japanese and Chinese populations were predicted using Simcyp's population library repository using the "Healthy-Volunteer", "Japanese" and "Chinese Healthy Volunteer" population models, respectively. Simulations for hepatic impairment were performed using Simulator's "Cirrhosis CP-A", "Cirrhosis CP-B" and "Cirrhosis CP-C" populations, while for renal impairment populations "RenalGFR\_30-60" and "RenalGFR\_less\_30" were used. The effects of age, race and organ impairment simulations were not simulated for baloxavir, remdesivir and large molecules, as adequate PBPK modelling was not possible due to limited data availability in the literature. Based on recent findings from the IQ consortium<sup>28</sup> the impact of renal impairment can be well predicted within 2-fold of observed PK (AUC) and for hepatic impairment >70% of the cases were predicted within 2-fold, supporting the utility of PBPK modelling for the study of organ dysfunction. Physiological differences between healthy volunteers and patients with hepatic organ impairment are shown in **Supporting Information Table S4**.

### 2.3 | Simulating lung concentration for COVID-19 drugs

The permeability-limited lung model is particularly suitable for modeling and simulating drug disposition within the lung mass compartment and ELF compartment, which are the target sites for antiviral effects. The methodology of simulating these concentrations has been applied previously to tuberculosis<sup>22</sup> and recently for three COVID-19 repurposed drugs.<sup>29</sup> In this work, lung ELF concentrations were simulated using the geriatric population within the PBPK simulator with age range from 65 to 95 years old, with 50% female subjects. The impact of reduced CYP3A expression in the liver and gut by 30% in the geriatric population was implemented as shown by Schwenger et al<sup>20</sup> for oncology subjects to reflect the CYP3A suppression by cytokines.

### 2.4 | PBPK simulation and comparison with observed clinical data

The predicted  $C_{max}$  and AUC in healthy subjects were compared to the observed data to ensure the suitability of the models for their intended use. Subsequently, the predicted  $C_{max}$  and AUC ratios of organ dysfunction (estimated as the ratio of predicted  $C_{max}$  and AUC of organ dysfunction relative to healthy populations) were compared with the observed organ dysfunction  $C_{max}$  and AUC ratios. Partition coefficients ( $K_p$ ) between lung tissue and plasma data were available in rats (as shown in **Supporting Information Table S2**). Rat tissue  $K_p$  values were compared to *in silico* predicted human  $K_p$  values, assuming the unbound distribution is independent of species.

### 2.5 | Sensitivity analyses with varying degrees of CYP suppression by cytokine storm

Sensitivity analysis, via Simcyp's sensitivity analysis tool, was performed to study the effect of AUC change with reduced CYP3A4 abundance in the liver and gut. Acalabrutinib, ibrutinib, dexamethasone and darunavir are sensitive CYP3A4 substrates (Table 2) so these were chosen for these sensitivity analyses. CYP3A4 abundance was varied, with values 10-90% lower than those observed in healthy volunteers.

### 2.6 | Nomenclature of targets and ligands

Key protein targets and ligands in this article are hyperlinked to corresponding entries in <http://www.guidetopharmacology.org>, the common portal for data from the IUPHAR/BPS Guide to PHARMACOLOGY, and are permanently archived in the Concise Guide to PHARMACOLOGY 2019/20.<sup>54</sup>

## 3 | RESULTS

### 3.1 | Cytokine levels in COVID-19 patients

Table 1 shows that in healthy individuals, serum IL-6 concentrations were reported to range from 1.3 to 10.3 pg/mL.<sup>18</sup> They rise to 2.6-123 pg/mL in some patient groups with inflammatory diseases, including obesity,<sup>55</sup> rheumatoid arthritis,<sup>56</sup> psoriasis<sup>57</sup> and cirrhosis.<sup>58</sup> A recent meta-analysis reported IL-6 levels in COVID-19 patients with complex clinical complications to be nearly 3-fold higher than in patients with few complications.<sup>8</sup> The average serum level of IL-6 across the six studies reported in this review was 65.5 pg/mL in patients with severe acute respiratory distress syndrome (SARDS), which is significantly higher than in nonsevere cases of disease (21.4 pg/mL) (Table 1). Mortality rates correlated with higher levels of IL-6, and the addition of IL-6 inhibitors such as tocilizumab improved clinical outcomes with no deaths in a total of 21 patients receiving treatment.<sup>8</sup> Similar results have been observed for acalabrutinib in COVID-19 patients; elevated IL-6 levels (median [range] of 44 [25-89.8] pg/mL) were noted in COVID-19 patients with a significant ( $P = 6.5 \times 10^{-4}$ ) decline observed during acalabrutinib treatment.<sup>3</sup>

### 3.2 | PK/PD of repurposed COVID-19 drugs

Table 2 summarizes the observed data for PK/PD properties of repurposed COVID-19 drugs. The half-maximal inhibitory concentration ( $IC_{50}$ ) parameters obtained were treated as unbound  $IC_{50}$  because the experimental conditions utilize serum-free conditions for COVID-19 drugs and this hypothesis was recently supported by Fan et al.<sup>59</sup> However, the *in vivo* plasma and lung tissue concentrations were corrected using *in silico* predicted tissue protein binding and measured plasma protein binding. The preclinical rat partition co-efficient ( $K_p$ ) values for lung tissue are compared with human predicted  $K_p$  values as listed in **Supporting Information Table S2**.

### 3.3 | ADME, DDIs and adverse events of repurposed COVID-19 drugs

Table 3 summarizes the main metabolizing enzymes, DDIs and AEs of repurposed COVID-19 drugs obtained from University of Washington Drug Interaction Database (DIDB) or New Drug Application (NDA) application information on FDA website. When repurposed COVID-19 drugs act as perpetrators: no clinically significant DDIs are anticipated except ritonavir, which is a well-known time dependent inhibitor of CYP3A4, and darunavir, which is a reversible CYP3A inhibitor; While, if these COVID-19 drugs act as a victim drugs: weak to moderate DDI risk is anticipated for COVID drugs that are mainly metabolized by CYP3A4 except ibrutinib. Strong DDI (>5-fold change in AUC) is anticipated for drugs that have a first-pass gut metabolism like ibrutinib when dosed with ritonavir.

**TABLE 2** Human PKPD properties of repurposed COVID-19 treatment

Drug	Target	Rationale	Target IC <sub>50</sub>	Dose and regimen	CL (L/h or L/h/kg)
Acalabrutinib	BTK inhibitor	BTK inhibition reduces production of cytokines and chemokines, including TNF- $\alpha$ , IL-6, IL-10 and MCP-1, which may contribute to exaggerated inflammatory responses to SARS-CoV-2 <sup>3</sup>	K <sub>d</sub> (derived from K <sub>inact</sub> and K <sub>in</sub> ) 3 nM	100 mg BID	CL/F = 159 L/h
Azithromycin	Anti-viral	Macrolide antibiotic with anti-viral properties. Has shown activity against rhinovirus, Zika and Ebola viruses in vitro <sup>30,31</sup> Prevents severe respiratory tract infections in patients suffering viral infection <sup>32</sup>		500 mg QD (2 $\times$ 250 mg)	CL <sub>iv</sub> = 37.8 L/h
Baloxavir	Antiviral	Polymerase acidic endonuclease inhibitor that interferes with replication; approved for use against influenza <sup>33</sup>	0.73 nM (n = 19; range: 0.20-1.85 nM) for subtype A/H1N1 strains, 0.68 nM (n = 19; range: 0.35-1.87 nM) for subtype A/H3N2 strains <sup>33</sup>	40 mg QD	CL/F = 10.3 L/h
Chloroquine	Antimalarial	Prevent virus entry into cells by interfering with angiotensin-converting enzyme 2 (ACE 2) receptor-mediated endocytosis	IC <sub>50</sub> against <i>P. falciparum</i> 3D7 (from three different assays): 7.69 $\pm$ 2.2 nM, 9.55 $\pm$ 3.1 nM, 7.01 $\pm$ 2.6 nM (7); IC50 against <i>P. falciparum</i> T996 and K1 are 18.5 nM and 264 nM <sup>34</sup>	300 mg QD (oral or IV)	CL/F = 0.5 L/h/kg
Hydroxychloroquine	Antimalarial	Accumulates in the lungs, where coronavirus collects <sup>35,36</sup>	IC50 against <i>P. falciparum</i> T996 and K1 are 21.5 nM and 22217 nM <sup>36</sup>	200 mg QD	CL/F = 10.9 L/h
Dapagliflozin	SGLT2 inhibitor	SGLT2 inhibition prevents severe clinical complications in patients with pre-existing conditions; dapagliflozin treatment is protective in patients with chronic kidney disease, type 2 diabetes or heart failure with reduced ejection fraction	IC <sub>50</sub> 1.12 nM for hSGLT2 <sup>37</sup>	10 mg QD	CLR = 13.93 L/h CL/F = 22.9 L/h
Lopinavir/ritonavir	Antiviral	HIV-1 protease inhibitor used with ritonavir for human immunodeficiency virus (HIV) infection	HIV IC <sub>50</sub> of $\sim$ 17 nM <sup>38</sup>	Lopinavir/ritonavir 400/100 mg oral BID	Lopinavir: 0.71 L/h/kg ritonavir: 0.52 L/h/kg

(Continues)

TABLE 2 (Continued)

Drug	Target	Rationale	Target IC <sub>50</sub>	Dose and regimen	CL (L/h or L/h/kg)
Ibrutinib	BTK inhibitor	BTK inhibition reduces production of cytokines and chemokines, including TNF $\alpha$ , IL-6, IL-10 and MCP-1, which may contribute to exaggerated inflammatory responses to SARS-CoV-2 <sup>4</sup>	K <sub>d</sub> (derived from K <sub>inact</sub> and K <sub>in</sub> ) 0.24 nM	420 mg QD	CL/F = 14.3 L/kg
Atazanavir	Antiviral	Shown to dock in the active site of SARS-CoV-2 Mpro, blocking Mpro activity Inhibits SARS-CoV-2 replication in vitro, either alone or in combination with ritonavir <sup>39</sup>	HIV 2.6-5.3 nM <sup>38</sup>	400 mg QD alone and 300 mg with 100 mg ritonavir QD	8.46 (CI: 6.12-10.9) L/h (after administration of atazanavir/ritonavir 300/100 mg QD in 24 HIV patients)
Darunavir	Antiviral	HIV protease inhibitor used to treat HIV infection in patients previously placed on antiretroviral therapies	HIV IC <sub>50</sub> : 1-2 nM <sup>38</sup>	Darunavir 600 mg/ritonavir 100 mg BID	IV admin.: 32.8 L/h alone and 5.9 L/h with ritonavir
Baricitinib	JAK inhibitor	JAK1/2 and AAK1 inhibition may alter inflammation and cellular viral entry in COVID-19 <sup>40</sup>	JAK1 IC <sub>50</sub> : 4 nM; JAK2: 6.6 nM; JAK3: 259 nM; TYK2: 21.1 nM <sup>41</sup>	4 mg QD in RA pts	8.9 L/h (patients)
Ruxolitinib	JAK inhibitor	JAK1/2 inhibition reduces production of proinflammatory cytokines like IL-6	JAK1 IC <sub>50</sub> : 0.09 nM; JAK2: 0.036 nM; JAK3: 2 nM; TYK2 IC <sub>50</sub> : 0.4 nM <sup>41</sup>	10, 30, 40 or 50 mg QD (2 x 5, 15, 20 or 25 mg) based on platelet count	19.2 L/h
Remdesivir	Antiviral	Adenosine analogue which gets incorporated into nascent viral RNA chains causing pre-mature termination <sup>42</sup> Inhibits the replication of multiple viruses, including SARS/MERS-CoV	Ituri ebola virus IC <sub>50</sub> : 12 nM; makona ebola virus 13 nM <sup>43</sup> Ebola virus IC <sub>50</sub> HeLA cells: 100 nM; ebola virus HMVEC cells: 53 nM; ebola macrophages: 86 nM <sup>44</sup>	75 mg IV dose infused over 30 min	NA
Dexamethasone	Immunosuppressant	Corticosteroid: binds to cytosolic glucocorticoid receptors, inhibiting nuclear factor NF- $\kappa$ B signalling, the mitogen-activated protein kinase (MAPK) pathway and downstream activator protein-1 (AP-1), preventing the production of inflammatory mediators such as interleukin-1 $\beta$ and tumor necrosis factor- $\alpha$ . <sup>45</sup>		20 or 40 mg once daily for tablet form	20 mg oral dose: 15.7 L/h 1.5 mg oral dose: 15.6 $\pm$ 4.9 L/h 3.0 mg intramuscular dose: 9.9 $\pm$ 1.4 L/h <sup>46</sup>

(Continues)

TABLE 2 (Continued)

Drug	Target	Rationale	Target IC <sub>50</sub>	Dose and regimen	CL (L/h or L/h/kg)
Tocilizumab <sup>47</sup> Phase III	Immunosuppressant	Human monoclonal antibody which binds to soluble and membrane-bound IL-6 receptor preventing IL-6 mediated inflammatory signalling <sup>48</sup> Retrospective studies of use in COVID-19 cases identified various clinical, laboratory and radiological improvements	2.5 × 10 <sup>-9</sup> – <sup>49</sup>	Dosed at 8 mg/kg, 400 mg and 80–600 mg across retrospective COVID-19 studies alongside other agents <sup>50</sup>	2.43E-04 (17%) L/h/kg Linear clearance in RA patients 0.0125 L/h, giant cell arteritis patients 6.7E-03 L/h, polyarticular juvenile idiopathic arthritis patients 5.8E-03 L/h, systemic juvenile idiopathic arthritis 5.7E-03 L/h
Sarilumab Phase II/III	Immunosuppressant	Human monoclonal antibody which binds membrane-bound and soluble human IL-6R $\alpha$ to prevent IL-6-mediated inflammatory signaling	54 pM		(Not eliminated via renal or hepatic pathways)
IFN- $\beta$ 1b (alone and with lopinavir-ritonavir, phase II) PK properties listed are for IFN $\beta$ -1b alone	Immunomodulator	Binds to type I interferon receptors (IFNAR1 and IFNAR2c), leading to the activation of immunomodulatory and antiviral proteins. Activity against SARS-CoV and MERS-CoV in vitro Has been shown to improve outcome of MERS-CoV infection in marmoset model. Chen et al 2015 Improved outcomes in patients with mild to moderate SARS-CoV-2 in combination with lopinavir and ritonavir. <sup>47</sup>	...		0.56–1.7 L/h/kg (in patients with diseases other than MS receiving single intravenous doses up to 2.0 mg)
IFN $\beta$ -1a (as inhaled SNG001) Phase II	Immunomodulator	See above		Activity against SARS in vitro <sup>51</sup>	33–55 L/h (healthy SC injection of 60 $\mu$ g)
Anakinra Phase III Tested alone and in combination with other drugs. <sup>52</sup>	Immunosuppressant	IL-1 receptor agonist which blocks the biological activity of IL-1 $\alpha$ and IL-1 $\beta$ <sup>50</sup>			(Variable, increases with increasing creatinine clearance and body weight, gender and age not significant factors) <sup>50</sup>
Siltuximab Phase III <sup>53</sup>	Antineoplastic agent	Monoclonal antibody against IL-6 to prevent inflammatory signalling	34 pM		9.58E-03 L/h

(Continues)



TABLE 2 (Continued)

Drug	Target	Rationale	Target IC <sub>50</sub>	Dose and regimen	CL (L/h or L/h/kg)
Leronlimab Phase II	Immunomodulator	Monoclonal antibody against CCR5 (C-C chemokine receptor type 5) CCR5; the downstream effects of CCR5 signalling include activation of NF- $\kappa$ B and IL-6 Granted emergency investigational new drug (EIND) status by the FDA for use in COVID-19 patients.			...
Ravulizumab Phase III	Terminal complement inhibitor	Amino-acid-substituted derivative of eculizumab (see below)	0.5 nM (binding to purified hC5 using surface plasmon resonance (SPR))		3.33E-03 L/h in PNH patients
Eculizumab Phase III	Terminal complement inhibitor	Monoclonal IgG antibody that binds complement protein C5 and prevents formation of membrane attack complex (MAC)	4.6 pM and 120 pM at 25 °C and 37 °C, respectively		2.6E-04 L/h/kg in RA patients

<sup>a</sup>AUC and C<sub>max</sub> are presented as unbound plasma values except for biologicals which are shown as total plasma values.

Abbreviations: AUC, area under the concentration-time curve; AUC<sub>INF</sub>, area under the concentration-time curve from time zero to infinity; BID, twice a day; CL, clearance; CLR, renal clearance; F, bioavailability; HIV, human immuno-deficiency virus; IC<sub>50</sub>, concentration required to reach half the maximum inhibitory effect; K<sub>inact</sub>, inactivation rate constant; K<sub>in</sub>, inhibition constant; K<sub>d</sub>, dissociation constant; NOMID, neonatal onset multisystem inflammatory disease; NA, Not Applicable; PNH, paroxysmal nocturnal haemoglobinuria; QD, once every day; RA, rheumatoid arthritis; SC, subcutaneous injection; V<sub>d</sub>, volume of distribution; V<sub>dss</sub>, volume of distribution at steady state.

TABLE 2 (Continued)

Drug	$V_d/F$ or $V_{dss}$ (L or L/kg)	AUC <sup>a</sup> (unbound) (ng.h/mL)	$C_{max}^a$ (unbound) (ng/mL)	Fraction unbound ( $f_u$ )
Acalabrutinib	34 L	28.9 ng.h/mL	8.4 ng/mL	0.026
Azithromycin	31.1 L/kg	AUC <sub>0-24</sub> = 1794 ng.h/mL	345 ng/mL	0.69
Baloxavir	1180 L	AUC <sub>INF</sub> = 400.4 ng.h/mL	6.27 ng/mL	0.065
Chloroquine	$V_d/F = 200$ L/kg	AUC = 9900 ng.h/mL (1 x 300 mg/week)	26-51.2 ng/mL	0.4
Hydroxychloroquine	Central $V_d = 733$ L, peripheral $V_d = 1.630$ L	AUC <sub>INF</sub> = 17179.8 ng.h/mL	204.9 ng/mL	0.5
Dapagliflozin	118 L	31.65 ng.h/mL	9.98 ng/mL	0.086
Lopinavir/ritonavir	Lopinavir: 0.8 L/kg Ritonavir: 0.6 L/kg	...	Ritonavir 7151.8 ng/mL Lopinavir 9580 ng/mL	Ritonavir 0.62
Ibrutinib	143 L/kg	16.8 ng.h/mL	4.4 ng/mL	0.027
Atazanavir	Atazanavir 1.6-2.7 L/kg	For 400 mg QD dose 4102.4 ng.h/mL For 300/100 Atazanavir/ritonavir QD 8600.9 ng.h/mL	For 400 mg QD dose 750.12 ng/mL For 300/100 atazanavir/ritonavir QD 903 ng/mL	Atazanavir 0.14
Darunavir	131 L		251.8 ng/mL	0.05
Baricitinib	76 L		26.7 ng/mL	0.5
Ruxolitinib	72 L (patients)		5.66 ng/mL for 20 mg QD 12.7 ng/mL for 50 mg QD	0.033
Remdesivir	Not reported, but expected to be equal to liver blood flow	240.7 ng.h/mL (27% CV)	196.7 ng/mL (38% CV)	0.121
Dexamethasone	A 1.5 mg oral dose: 51.0 L, 3 mg intramuscular dose: 96.0 L <sup>46</sup>	(AUC <sub>INF</sub> ) 1271 ng.h/mL	247 ng/mL	0.28
Tocilizumab <sup>47</sup> Phase III	$V_{ss} = 6.4$ L in RA patients, FDA: giant cell arthritis patients 7.46 L, paediatric patients with polyarticular juvenile arthritis 4.08 L, paediatric patients with systemic juvenile idiopathic arthritis 4.01 L	RA patients: 162 mg (subcutaneous) weekly: 8 254 000 ± 3 833 000 ng.h/mL 162 mg every 2 weeks 3 460 000 ± 2 530 000 ng.h/mL 162 mg every 4 weeks: 39 216 000 ± 14 304 000 ng.h/mL <sup>48</sup>	RA patients: 242000 ng/mL 162 mg weekly: 51 300 ± 23 200 ng/mL 162 mg every 2 weeks 13 000 ± 8300 ng/mL 162 mg every 4 weeks: 154 000 ± 42 000 ng/mL <sup>48</sup>	
Sarilumab Phase II/III	7.3 L in RA patients	150 mg dosing (every 2 weeks): 8416.6 ± 5000 ng.h/mL 200 mg dosing (every 2 weeks): 16458.3 ± 8625 ng.h/mL	150 mg dosing (every 2 weeks): 20000 ± 9200 ng/mL 200 mg dosing (every 2 weeks): 600 ± 15 200 ng/mL	
IFN-B 1b (alone and with lopinavir-ritonavir, phase II) PK properties listed are for IFNB-1b alone	0.25-2.88 L/kg	...	...	

(Continues)

TABLE 2 (Continued)

Drug	$V_d/F$ or $V_{dss}$ (L or L/kg)	AUC <sup>a</sup> (unbound) (ng.h/mL)	$C_{max}$ <sup>a</sup> (unbound) (ng/mL)	Fraction unbound ( $f_u$ )
IFN $\beta$ -1a (as inhaled SNG001) Phase II	Not available	Not available	Not available	
Anakinra Phase III Tested alone and in combination with other drugs. <sup>52</sup>	-	...	(SC dose of 3 mg/kg once daily NOMID patients) 3628 (655-8511) ng/mL. <sup>50</sup>	
Siltuximab Phase III <sup>53</sup>	(70 kg male subject) is 4.5 L		332 000 ng/mL (11 mg/kg, once every 3 weeks in patients with multicentric Castleman's disease)	
Leronlimab Phase II	...	162 mg subcutaneous dose: 2183.3 ng.h/mL 324 mg subcutaneous dose: 2450 ng.h/mL	162 mg subcutaneous dose: 6100 ng/mL 324 mg subcutaneous dose: 13800 ng/mL	
Ravulizumab Phase III	5.34 (0.92) L			
Eculizumab Phase III	5-8 L	2.45E+07 ng.h/mL	194 000 $\pm$ 76 000 ng/mL	

<sup>a</sup>AUC and  $C_{max}$  are presented as unbound plasma values except for biologicals which are shown as total plasma values.

Abbreviations: AUC, area under the concentration-time curve; AUC<sub>INF</sub>, area under the concentration-time curve from time zero to infinity; BID, twice a day; CL, clearance; CLR, renal clearance; F, bioavailability; HIV, human immuno-deficiency virus; IC<sub>50</sub>, concentration required to reach half the maximum inhibitory effect;  $K_{inact}$ , inactivation rate constant;  $K_{in}$ , inhibition constant;  $K_{dt}$ , dissociation constant; NOMID, neonatal onset multisystem inflammatory disease; NA, Not Applicable; PNH, paroxysmal nocturnal haemoglobinuria; QD, once everyday; RA, rheumatoid arthritis; SC, subcutaneous injection;  $V_d$ , volume of distribution;  $V_{dss}$ , volume of distribution at steady state.

**TABLE 3** Metabolic pathway, DDI risk and adverse events

Drug	% contribution of metabolizing enzymes	Metabolizing enzyme inhibition/induction	Transporter inhibition/induction	Known DDI risk	Known adverse reactions (FDA label)
Acalabrutinib	CYP3A4 (80%) Renal (2%) Additional HLM (18%)	Reversible inhibition (K <sub>i</sub> ): CYP2C8 20.6 μM, CYP2C9 11.3 μM, CYP3A4/5 23.9 μM Mechanism-based inhibition: CYP3A4/5 K <sub>i</sub> (10.1 μM), K <sub>inact</sub> (1.11/h)	Not available	Higher risk as substrate (with strong CYP3A inhibitor), low risk as perpetrator	Anaemia, thrombocytopenia, headache, neutropenia, diarrhoea, fatigue, myalgia, bruising, nausea, abdominal pain, constipation, vomiting, rash, haemorrhaged/hematoma, serious infections, secondary primary malignancies, atrial fibrillation and flutter, epistaxis <sup>60</sup>
Azithromycin	Renal (18%) Biliary CL (82%)	CYP3A4 (weak) reversible inhibition IC <sub>50</sub> = 56 μM, mechanism-based inhibition: 3.18 × 10 <sup>-5</sup> /min/μM	P-gp IC <sub>50</sub> = 21.8 μM	No DDI with chloroquine (1000 mg) or digoxin, 25% increase in midazolam AUC	Nausea, diarrhoea, abdominal pain, vomiting, rash, pruritis, elevated ALT/AST, pain at injection site, local inflammation, vaginitis, anorexia, serious allergic reactions, hepatotoxicity, QT prolongation, infantile hypertrophic pyloric stenosis, exacerbation of myasthenia gravis, development of drug-resistant bacteria <sup>61</sup>
Baricitinib	Renal (80%) Additional CL (14%) CYP3A4 (6%)	Did not inhibit CYP1A2, CYP2B6, CYP2C8, CYP2C9, CYP2C19 or CYP2D6	OAT3 (IC <sub>50</sub> = 8.4 μM), OCT1 (IC <sub>50</sub> = 6.9 μM), OCT2 (IC <sub>50</sub> = 11.6 μM), OATP1B3 (IC <sub>50</sub> = 49.4 μM), MATE1 (IC <sub>50</sub> = 76.7 μM), and MATE2-K (IC <sub>50</sub> = 13.7 μM)	No DDI risk	Upper respiratory tract infections, serious infections, malignancy and lymphoproliferative disorders, thrombosis, GI perforations, neutropenia, lymphopenia, anaemia, liver enzyme elevations, lipid elevations, nausea, herpes simplex, and herpes zoster <sup>62</sup>
Baloxavir	Esterase, arylacetamide deacetylase and CYP3A4	Did not inhibit CYP1A2, CYP2B6, CYP2C8, CYP2C9, CYP2C19 or CYP2D6	Not available	No DDI with midazolam (CYP3A), digoxin (P-gp), rosuvastatin (BCRP)	Bronchitis, diarrhoea, nausea, nasopharyngitis and headache <sup>63</sup>
Chloroquine	CYP3A4 (23%) CYP2C8 (14%) Additional HLM (9%) Renal (54%)	Reversible inhibition: CYP2D6 (K <sub>i</sub> = 12 μM)	OATP1A2 (IC <sub>50</sub> = 20.5 μM)	Reduced bioavailability of ampicillin, increase exposure of cyclosporine	Cardiac (cardiomyopathy, QT interval prolongation, torsades de pointes, ventricular arrhythmias, hypotension, ECG changes, conduction disorders), hypoglycaemia, ocular (retinopathy,

(Continues)

TABLE 3 (Continued)

Drug	% contribution of metabolizing enzymes	Metabolizing enzyme inhibition/induction	Transporter inhibition/induction	Known DDI risk	Known adverse reactions (FDA label)
					maculopathy, macular degeneration, etc), acute extrapyramidal disorders, worsening of psoriasis/porphyria, potential carcinogenic risk, immune (urticaria, anaphylactic reaction including angioedema), nerve type deafness, tinnitus, reduced hearing in patients with preexisting auditory damage, sensorimotor disorders, skeletal muscle myopathy/neuromyopathy, hepatitis, increased liver enzymes, anorexia, nausea, vomiting, diarrhoea, abdominal cramps assorted skin and subcutaneous tissue disorders, pancytopenia, aplastic anaemia, reversible agranulocytosis, thrombocytopenia, neutropenia Haemolytic anaemia in G6PD-deficient patients, convulsions, mild/transient headache, polynuropathy, psychosis, delirium, anxiety, agitation, insomnia, confusion, hallucinations, personality changes, depression, suicidal behavior <sup>64</sup>
Hydroxychloroquine	Additional HLM (62%) Renal (38%)	Reversible inhibition: CYP2D6	OATP1A2 (IC <sub>50</sub> = 11.26 μM)	65% increase in metoprolol (CYP2D6) exposure, increase digoxin exposure	Ocular (irreversible retinopathy, visual field defects/disturbances, maculopathies, corneal changes, etc), QT prolongation (ventricular arrhythmias, torsades de pointes), ECG abnormalities, cardiomyopathy, worsening of psoriasis/porphyria, proximal

(Continues)

TABLE 3 (Continued)

Drug	% contribution of metabolizing enzymes	Metabolizing enzyme inhibition/induction	Transporter inhibition/induction	Known DDI risk	Known adverse reactions (FDA label)
Darunavir	CYP3A (66%) Additional HLM (33%) Renal (1%)	CYP3A4 (Ki = 0.4 µM) CYP2C9 (Ki = 52 µM) CYP2C19 (Ki = 25 µM)	Not available	Strong DDI risk with sensitive CYP3A substrates (>5-fold AUC ration change)	myopathy/neuropathy, suicidal behaviour, hypoglycaemia, bone marrow failure, anaemia, aplastic anaemia, agranulocytosis, leukopenia, thrombocytopenia, haemolysis (patients with G6PD deficiency), vertigo, tinnitus, nystagmus, nerve deafness, deafness, nausea, vomiting, diarrhoea, abdominal pain, fatigue, abnormal liver function tests, acute hepatic failure, urticaria, angioedema, bronchospasm, decreased appetite, porphyria, decreased weight, sensorimotor disorder, headache, dizziness, seizure, ataxia, extrapyramidal disorders, affect/emotional lability, nervousness, irritability, nightmares, psychosis, assorted skin and subcutaneous tissue disorders <sup>65</sup>
Dapagliflozin	CYP3A4 (9%) UGT1A9 (80%) UGT2B7 (9%) Renal (2%)	Not available	Not available	No significant DDI risk	Female and male genital mycotic infections, nasopharyngitis, urinary tract infections, back pain, increased urination, nausea, influenza, dyslipidaemia, constipation, discomfort with urination, pain in extremity, osmotic diuresis causing reductions in intravascular volume (dehydration, hypovolemia, orthostatic hypotension, hypotension), hypoglycaemia, hypersensitivity reactions, ketoacidosis, increase in serum

(Continues)

TABLE 3 (Continued)

Drug	% contribution of metabolizing enzymes	Metabolizing enzyme inhibition/induction	Transporter inhibition/induction	Known DDI risk	Known adverse reactions (FDA label)
Dexamethasone	Mainly CYP3A4 Renal <10%	Weak CYP3A induction	Dual roles in hOAT3 transport activity: when briefly incubated with hOAT3-expressing HEK293 cells, dexamethasone is a competitive inhibitor for hOAT3-mediated transport. IC50 = 49.91 µM, Ki = 47.08 µM, whilst prolonged incubation with dexamethasone upregulates hOAT3 expression and transport activity (Wang, Liu, you; 2018)	DDI with strong CYP3A4 inhibitors or inducers In addition, concomitant therapies such as erythropoietin stimulating agents or estrogenic containing therapies may increase the risk of thromboembolism (FDA label)	creatinine, haematocrit, LDL, decrease in eGFR, serum bicarbonate, acute kidney injury/intravascular volume contraction, necrotizing fasciitis of the perineum <sup>67</sup> Systemic fungal infections and hypersensitivity to dexamethasone (FDA label)
Ibrutinib	CYP3A (93%) Additional HLM (7%) <sup>68</sup>	No inhibition	P-gp IC50 = 5.67 µM	Sensitive CYP3A substrate Significant DDI risk with CYP modulators <sup>68</sup>	Neutropenia, thrombocytopenia, diarrhoea, anaemia, musculoskeletal pain, rash, nausea, bruising, fatigue, haemorrhaged and pyrexia <sup>69</sup>
Remdesivir	Mainly by phosphatase, remdesivir is 74% eliminated in the urine and 18% eliminated in the faeces	Remdesivir is an inhibitor of CYP3A4	Remdesivir is a substrate of OATP1B1 and P-gp. Remdesivir is an inhibitor of OATP1B1, OATP1B3, BSEP, MRP4 and NTCP in vitro	Due to its rapid clearance, DDI liability as perpetrator is limited	Limited clinical data available Infusion-related reactions, increased risk of transaminase elevations <sup>70</sup>
Ruxolitinib	CYP2C9 (38%) CYP3A4 (55%) Additional HLM (7%)	Reversible inhibition CYP3A4 Ki = 8.8 µM; weak CYP3A4 induction 10.1-fold at 30 µM	Not available	No DDI risk	Thrombocytopenia, anaemia, neutropenia, bruising, dizziness, headache, urinary tract infections, weight gain, flatulence, herpes zoster, alanine transaminase abnormalities, aspartate transaminase abnormalities, cholesterol elevation <sup>71</sup>

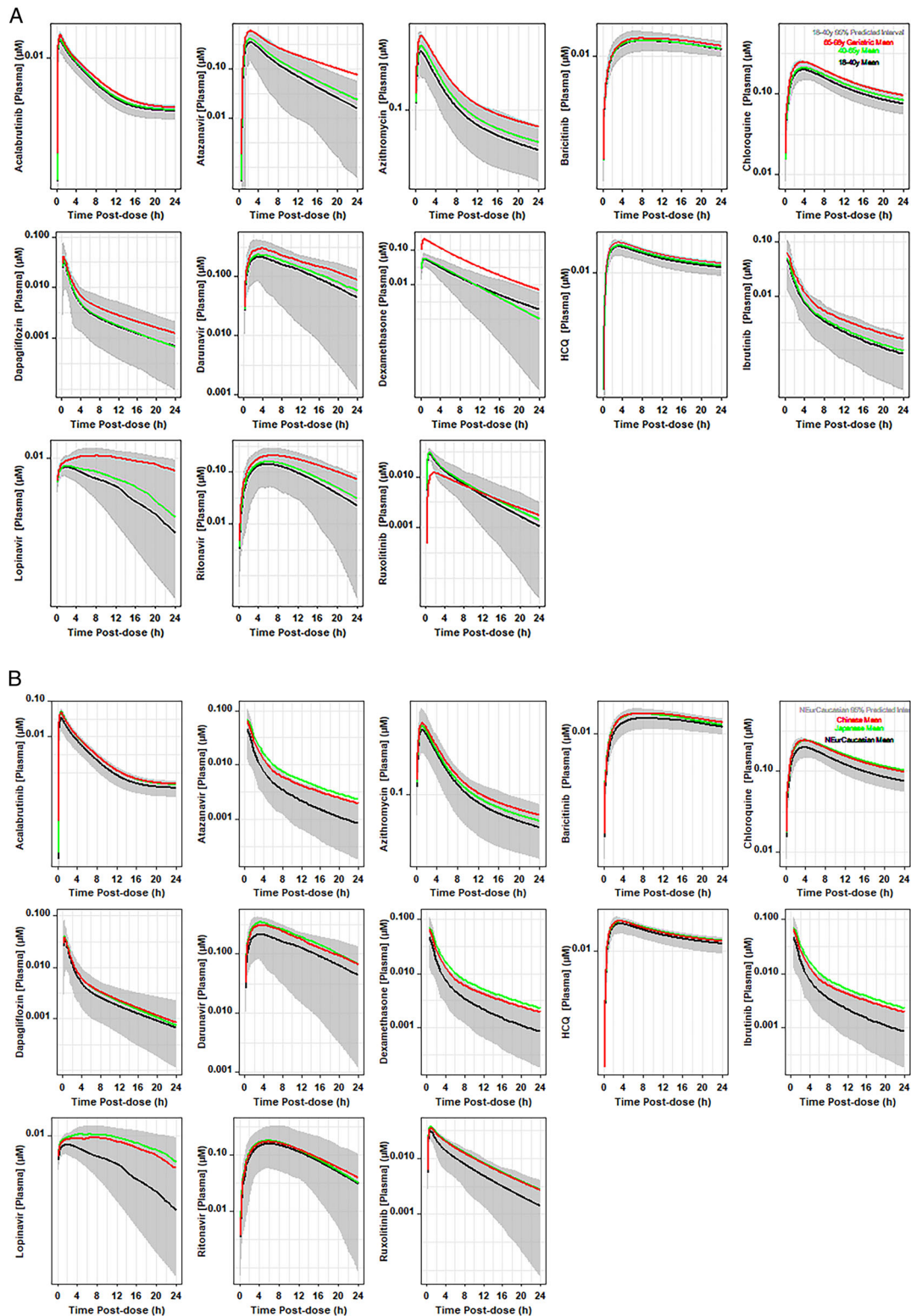
(Continues)

TABLE 3 (Continued)

Drug	% contribution of metabolizing enzymes	Metabolizing enzyme inhibition/induction	Transporter inhibition/induction	Known DDI risk	Known adverse reactions (FDA label)
Ritonavir	CYP2D6 (1%) CYP3A4 (81%) CYP3A5 (5%) Additional HLM (11%) Renal (2%)	Reversible inhibition (Ki): CYP2D6 0.04 $\mu$ M, CYP3A4 0.00194 $\mu$ M; mechanism based inhibition: CYP3A4/5 Ki (0.18 $\mu$ M), $K_{inact}$ (19.8/h)	P-gp IC50 = 0.03 $\mu$ M	Strong DDI with CYP3A substrates	Gastrointestinal (diarrhoea, nausea, vomiting, upper and lower abdominal pain, dyspepsia, flatulence, GI haemorrhage), GERD), neurological disturbances (paraesthesia and oral paraesthesia), rash and fatigue/asthenia, blurred vision, blood bilirubin increased (including jaundice), hepatitis (increased AST, ALT, GGT), hypersensitivity (including urticaria and face oedema), oedema and peripheral oedema, gout, hypercholesterolemia, hypertriglyceridemia, lipodystrophy acquired, arthralgia and back pain, myopathy/creatinine phosphokinase increased, myalgia, dizziness, dysgeusia, peripheral neuropathy, syncope, confusion, disturbance in attention, increased urination, coughing, oropharyngeal pain, acne, pruritus, flushing/feeling hot, hypotension, hypotension (including orthostatic hypotension), peripheral coldness and low haematocrit, haemoglobin, neutrophil, RBC, WBC <sup>72</sup>

Abbreviations: ALT, Alanine transaminase; AST, Aspartate transaminase; AUC, Area under the concentration-time curve; CL, Clearance; DDI, Drug-drug interaction; G6PD, Glucose-6-phosphate dehydrogenase; GERD, Gastroesophageal reflux disease; GGT, Gamma-glutamyl transferase; GI, Gastrointestinal; HLM, Human liver microsomes; IC50, The half maximal inhibitory concentration; Ki and K<sub>i</sub>, Inhibitor constants for reversible and irreversible inhibitions, respectively; RBC, Red blood cells; WBC, White blood cells.





**FIGURE 2** Effect of age (A) and race (B) on unbound plasma concentration-time profiles of COVID-19 drugs. (A) The black continuous line represents the median prediction using the PBPK model for 18-40 years of age, the green line for 40-65 years and the red line for 65-98 years. The shaded area represents the 95% prediction intervals of Caucasian healthy volunteers. (B) The black continuous line represents the median prediction using the PBPK model for Caucasians subjects, the green line for Japanese subjects and the red line for Chinese patients. Different race simulations were run using 40-65 years of age with 50% of females. Doses used: acalabrutinib 100 mg single dose, azithromycin 500 mg single dose, chloroquine 600 mg single dose, dapagliflozin 10 mg single dose, darunavir 800 mg single dose, hydroxychloroquine (HCQ) 200 mg single dose, ibrutinib 140 mg single dose, lopinavir 400 mg single dose (with 100 mg ritonavir concomitant interaction), rifampicin 600 mg single dose, baricitinib 2 mg single dose, ritonavir 600 mg single dose, ruxolitinib 20 mg single dose

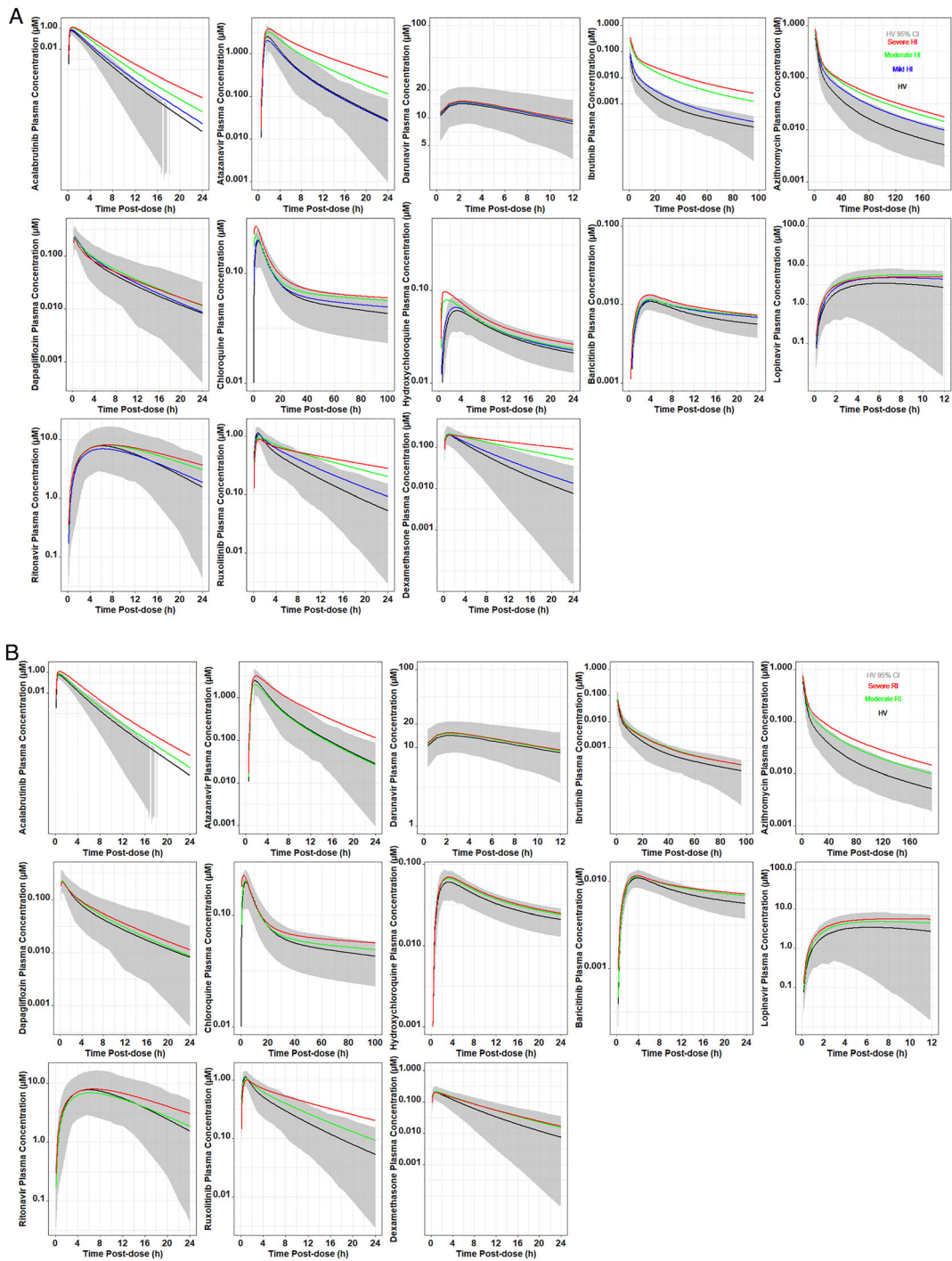


**FIGURE 3** Effect of hepatic (A) and renal (B) impairments on total plasma concentration-time profiles of COVID-19 drugs. The black continuous line represents the median prediction using the PBPK model for healthy population. The shaded area represents the 95% prediction intervals of the healthy population. The blue line represents mild hepatic impairment. The green line represents moderate renal or hepatic impairment. The red line represents severe renal or hepatic impairment. Doses used for hepatic impairment: acalabrutinib 50 mg single dose, azithromycin 500 mg single dose, atazanavir 400 mg single dose, chloroquine 300 mg single dose, dapagliflozin 10 mg single dose, hydroxychloroquine base (HCQ) 155 mg single dose, baricitinib 4 mg single dose, ritonavir 600 mg single dose, ruxolitinib 25mg single dose, lopinavir 400 mg single dosing interval (with 100 mg ritonavir concomitant interaction), darunavir 600 mg single dosing interval (with 100 mg ritonavir concomitant interaction), ibrutinib 140 mg single dose, dexamethasone 8 mg single dose. Only the parent acalabrutinib was measured in organ dysfunction or DDI studies of acalabrutinib. Doses used for renal impairment: azithromycin 500 mg single dose, atazanavir 400 mg single dose, hydroxychloroquine base 155 mg, baricitinib 4 mg single dose, chloroquine 300 mg single dose, dapagliflozin 50 mg single dose, acalabrutinib 50 mg single dose, ruxolitinib 25mg single dose, ritonavir 600 mg single dose, lopinavir 400 mg single dose (with 100 mg ritonavir concomitant interaction), darunavir 600 mg single dosing interval (with 100 mg ritonavir concomitant interaction), dexamethasone 8 mg single dose

**TABLE 4** Comparison of the predicted vs observed AUC ratios of hepatic impairment condition to matched healthy subjects for COVID-19 drugs

Drug	Drug dose/regimen in the study	Observed AUCR	Predicted AUCR	Observed ratio change in $C_{max}$ (diseased to healthy)	FDA dosage recommendation	Reference
Acalabrutinib	50 mg SD	CP-A: 1.9	CP-A: 1.35	CP-C: 4.9	No dose adjustment for CP-A and CP-B patients Avoid dosing acalabrutinib in CP-C	73
		CP-B: 1.5	CP-B: 2.76			
		CP-C: 5.3	CP-C: 3.41			
Ibrutinib	140 mg SD	CP-A: 2.7	CP-A: 1.7	CP-A: 5.2	140 mg daily for CP-A patients, 70 mg daily for patients with CP-B and should be avoided in CP-C	74
		CP-B: 8.2	CP-B: 6.9	CP-B: 8.8		
		CP-C: 9.8	CP-C: 9.9	CP-C: 7		
Azithromycin	500 mg SD	CP-A: 0.98	CP-A: 1.5	CP-A: 1.34	No need to change in CP-A and CP-B The pharmacokinetics of azithromycin in subjects with severe HI have not been established	75
		CP-B: 0.82	CP-B: 1.6	CP-B: 1.76		
		CP-C: N/A	CP-C: 2.2	CP-C: N/A		
Baloxavir	40 mg SD	CP-B: 1.12	N/A	CP-B: 0.8	No dose adjustment is needed for subjects with CP-A and CP-B Studies on mild HI was not conducted because no clinically meaningful effect was observed in the moderate condition The pharmacokinetics in patients with severe HI have not been evaluated	33
Chloroquine	300 mg SD	N/A	CP-A: 1.42 CP-B: 1.93 CP-C: 2.15	N/A	It should be used with caution in patients with HI or alcoholism	76
Hydroxychloroquine	155 mg SD	N/A	CP-A: 1.12 CP-B: 1.25 CP-C: 1.34	N/A	Should be used with caution in patients with HI or alcoholism or in conjunction with known hepatotoxic drugs A reduction in dosage may be necessary in patients with HI, as well as in those taking medicines known to affect the liver	77
Dapagliflozin	10 mg SD	CP-A: 1.03	CP-A: 1.08	CP-A: 0.88	No dose adjustment is recommended for patients with mild, moderate or severe HI However, the benefit-risk for the use of dapagliflozin in patients with severe HI should be individually assessed since the safety and efficacy of dapagliflozin	67
		CP-B: 1.36	CP-B: 1.19	CP-B: 1.12		
		CP-C: 1.67	CP-C: 1.1	CP-C: 1.4		

(Continues)

TABLE 4 (Continued)

Drug	Drug dose/regimen in the study	Observed AUCR	Predicted AUCR	Observed ratio change in $C_{max}$ (diseased to healthy)	FDA dosage recommendation	Reference
Baricitinib	4 mg SD	CP-B: 1.19	CP-A: 1.38 CP-B: 1.37 CP-C: 1.31	CP-B: 1.08	have not been specifically studied in this population No dose adjustment is necessary in patients with mild or moderate HI The use of baricitinib has not been studied in patients with severe HI and is therefore not recommended	78
Lopinavir	400 mg with 100 mg ritonavir BID	CP-A: 1.367 CP-B: 1.229	CP-A: 1.14 CP-B: 1.496 CP-C: 1.39	CP-A: 1.25 CP-B: 1.16	The change in exposure in mild and moderate HI is not expected to be clinically relevant Lopinavir has not been studied in patients with severe hepatic impairment	79
Atazanavir	400 mg SD	CP-B&-C: 1.42	CP-A: 0.87 CP-B: 1.93 CP-C: 2.95	N/A	Dose reduction to 300 mg per day is recommended in moderate HI	80
Darunavir	600 mg darunavir/100 mg ritonavir twice daily	CP-A: 0.94 (0.75-1.17 90% CI) CP-B: 1.2 (0.9-1.6 90% CI)	CP-A: 1.04 CP-B: 1.06 CP-C: 1.07	CP-A: 0.88 (0.73-1.07) CP-B: 1.22 (0.95-1.56)	No significant change in dose for moderate cirrhosis Not studied in severe HI	81
Ruxolitinib	25 mg SD	CP-A: 1.87 (90% CI 1.29-2.71) CP-B: 1.28 (0.88-1.85) CP-C: 1.65 (1.14-2.4)	CP-A: 1.31 CP-B: 2.04 CP-C: 2.67	CP-A: 0.92 (0.66-1.29) CP-B: 0.78 (0.56-1.1) CP-C: 0.85 (0.6-1.19)	Reduce dose is recommended in patients with any HI	82
Ritonavir	600 mg SD	CP-A: 1.26 CP-B: 0.93	CP-A: 1.014 CP-B: 1.44 CP-C: 1.66	CP-A: 1.12 CP-B: 0.56	No dose adjustment of ritonavir is necessary for patients with either mild or moderate HI No pharmacokinetic or safety data are available regarding the use of ritonavir in subjects with CP-C, therefore ritonavir is not recommended for use in patients with severe HI	79
Remdesivir	Day 1: SD 200 mg IV days 2-10: 100 mg/day	N/A	N/A	N/A	The pharmacokinetics and dosage adjustment of remdesivir have not been evaluated in patients with HI Hepatic laboratory testing should be performed in all patients prior to starting	70

(Continues)

**TABLE 4** (Continued)

Drug	Drug dose/regimen in the study	Observed AUCR	Predicted AUCR	Observed ratio change in $C_{max}$ (diseased to healthy)	FDA dosage recommendation	Reference
Dexamethasone	8 mg SD	N/A	CP-A: 1.20 CP-B: 2.06 CP-C: 2.56	N/A	remdesivir and daily while receiving remdesivir The effect of baseline HI on the pharmacokinetics of dexamethasone has not been studied clinically	<sup>83</sup>

Abbreviations: AUCR, ratio of the area under total plasma concentration-time curve in diseased population relative to healthy population; BID, Twice a day; CI, confidence interval;  $C_{max}$ , maximum plasma concentration; CP-A, CP-B, CP-C, child Pugh classification of cirrhosis A (mild), B (moderate), C (severe); HI, hepatic impairment; IV, intravenous; N/A, not available; SD, single oral dose.

### 3.4 | Effect of age and race on PK of repurposed COVID-19 drugs

Figure 2A shows the PBPK model simulated PK profiles for different age brackets: 18-40 years, 40-65 years and 65-98 years (geriatric population). These age brackets represented the typical demographics from a recent remdesivir clinical trial.<sup>2</sup> We assumed the proportion of females in the simulations to be 50%. The PBPK model-based results are in line with observed data, as shown in **Supporting Information Table S3**. The geriatric population exhibited higher exposure for all drugs compared to the age bracket of 18-40 years, but fell within the 95% prediction intervals (PIs) of healthy volunteers except for dexamethasone, which is marginally outside the shaded area of the 95% PI (Figure 2A). PBPK analysis suggests race has no clinically meaningful effect on the clearance of all COVID-19 drugs, as the mean simulated Chinese and Japanese population profiles fall within the 95% PI of the Caucasian population (Figure 2B), therefore no dose adjustment is required based on the race of the patient.

### 3.5 | Effect of organ dysfunction on PK of repurposed COVID-19 drugs

Comparing predicted AUCR ( $AUC_{0-\infty}$  in hepatic or renal impairment/ $AUC_{0-\infty}$  in healthy volunteers) with their corresponding observed values (whenever available) shows consistency within 2-fold of observed data for all drugs, suggesting the developed PBPK models were adequate to simulate the exposure changes where a clinical data gap exists. Figure 3A,B and Table 4 show how hepatic impairment resulting from cirrhosis and renal impairment (Table 5) change the exposure levels of these repurposed drugs. The absolute expression of CYP3A levels in mild to severe cirrhotic or renal failure subjects vs the healthy population within the Simcyp PBPK Simulator V19 is shown in **Supporting Information Tables S4** and **S5**. In addition, physiological differences between either liver cirrhosis or renal impairment populations vs the healthy population is also described. The exposure of azithromycin, atazanavir,

acalabrutinib, ruxolitinib and dexamethasone was clearly higher in severe hepatic impairment (Figure 3A) relative to healthy volunteers, suggesting the need for dose adjustment. In the case of renal impairment (Figure 3B), ruxolitinib, atazanavir and azithromycin plasma exposures were higher in severe conditions relative to healthy population and may warrant a dose adjustment in severely renally impaired patients.

### 3.6 | Simulating target site concentration for COVID-19 drugs

Figure 4 shows the simulated relative exposure of lung to plasma at steady state, depicting unbound ELF concentrations in the geriatric population aged from 65 to 95 years along with 95% PIs. The horizontal dashed lines show the  $IC_{50}$  and  $IC_{90}$  ( $9 \times IC_{50}$ ) range of target inhibition. The input parameters used for the permeability-limited lung model<sup>22</sup> are shown in **Supporting Information Tables S1** and **S2**. Overall, all COVID-19 drugs appear to reach adequate exposures at steady state over the target  $IC_{50}$  values of respective drugs and stay above this for a minimum of 8 hours except for all antiviral drugs, where reported  $IC_{50}$  values against SARS-CoV-2 were reported.<sup>88</sup> Nevertheless, the antiviral exposures were above  $IC_{50}/IC_{90}$  if human immunodeficiency virus (HIV) target values were used. Achieving 90% of target inhibition with unbound ELF concentration in most patients is achievable for a period of time (>4 hours; Figure 4) except for all antiviral drugs and the hydroxychloroquine potency value ( $IC_{50}$  in the range of 13-119  $\mu$ M) reported recently by Hoffman et al in SARS-CoV-2 relevant Vero and Calu-3 cell lines.<sup>89</sup> Under the assumption that in vivo cellular accumulation is similar to that from the in vitro studies, the calculated free lung concentrations in the ELF that would result from proposed dosing regimens are well below the in vitro  $IC_{50}/IC_{90}$  value, making the antiviral effect against SARS-CoV-2 not likely achievable with an oral dosing regimen of hydroxychloroquine. Total (parent + metabolite) unbound plasma and ELF concentration were used to estimate an average BTK occupancy for acalabrutinib (a covalent BTK binder). Estimated BTK occupancy was >95%, which

**TABLE 5** Comparison of the predicted vs observed AUC ratios of renal impairment condition to matched healthy subjects for COVID-19 drugs

Drug	Drug dose/regimen in the study	Average observed ratio of change in AUC	Average predicted ratio of change in AUC	Observed ratio change in $C_{max}$	FDA dosage recommendation
Acalabrutinib	50 mg SD	N/A	Moderate RI: 1.33 Severe RI: 1.2	N/A	No clinically relevant PK difference was observed in patients with mild or moderate renal impairment (eGFR $\geq 30$ mL/min/1.73m <sup>2</sup> , as estimated by MDRD) Acalabrutinib PK has not been evaluated in patients with severe renal impairment (eGFR $< 29$ mL/min/1.73m <sup>2</sup> MDRD) or renal impairment requiring dialysis
Azithromycin	500 mg SD	Mild to moderate RI: 1.04 Severe RI: 1.35	Moderate RI: 1.46 Severe RI: 1.72	Mild to moderate RI: 1.05 Severe RI: 1.61	No dose adjustment
Baloxavir	40 mg SD	N/A	N/A	N/A	Pop-PK analysis did not identify any clinically meaningful effect of renal function on the pharmacokinetics of baloxavir in patients with creatinine clearance (CrCl) 50 mL/min and above No studies on severe RI
Chloroquine	300 mg SD	N/A	Moderate RI: 1.74 Severe RI: 2.15	N/A	Extra caution should be exercised when prescribing chloroquine for prolonged use in patients with renal insufficiency
Hydroxychloroquine	155 mg SD	N/A	Moderate RI 1.16 Severe RI: 1.17	N/A	A reduction in dosage may be necessary in patients with renal disease, as well as in those taking medicines known to affect the kidneys
Dapagliflozin	50 mg SD	T2DM with: Mild RI: 1.28 Moderate RI: 1.52 Severe RI: 1.75	Moderate RI: 1.24 Severe RI: 1.11	T2DM with: Mild RI: 1.14 Moderate RI: 1.26 Severe RI: 1.36	No dose adjustment is needed in patients with an eGFR greater than or equal to 45 mL/min/1.73 m <sup>2</sup> Not recommended when the eGFR is less than 45 mL/min/1.73 m <sup>2</sup> Contraindicated in patients with an eGFR less than 30 mL/min/1.73 m <sup>2</sup>
Baricitinib	4 mg SD	Mild RI: 1.41 Moderate RI: 2.22 Severe RI: 4.05 ESRD: 2.41	Moderate RI: 1.63 Severe RI: 2.03	Mild RI: 1.16 Moderate RI: 1.46 Severe RI: 1.4 ESRD: 0.88	Renal impairment renal function was found to significantly affect baricitinib exposure It is not recommended for use in patients with estimated GFR of less than 60 mL/min/1.73 m <sup>2</sup>
Lopinavir	400 mg lopinavir + 100 mg ritonavir BID	N/A	Moderate RI: 1.092 Severe RI: 0.94	N/A	Lopinavir pharmacokinetics have not been studied in patients with renal impairment; however, since the renal clearance of lopinavir is negligible, a decrease in total body clearance is not

(Continues)

TABLE 5 (Continued)

Drug	Drug dose/regimen in the study	Average observed ratio of change in AUC	Average predicted ratio of change in AUC	Observed ratio change in $C_{max}$	FDA dosage recommendation
Atazanavir	400 mg once daily	Severe RI without dialysis AUC: 1.19 Severe RI with haemodialysis AUC: 0.57-0.75	Moderate RI: 1.49 Severe RI: 2.27	Severe RI without dialysis, $C_{max}$ : 0.91 Severe RI with haemodialysis, $C_{max}$ : 0.75	expected in patients with renal impairment It is not recommended for use in HIV-treatment-experienced patients with end-stage renal disease managed with haemodialysis
Darunavir	800 mg SD	N/A	Moderate RI: 1.39 Severe RI: 1.84	N/A	Renal impairment: not studied Population pharmacokinetic analysis showed that the pharmacokinetics of darunavir were not significantly affected in HIV-infected subjects with moderate renal impairment (CrCL between 30-60 mL/min, n = 20) No pharmacokinetic data are available in HIV-1-infected patients with severe renal impairment or end stage renal disease; however, because the renal clearance of darunavir is limited, a decrease in total body clearance is not expected in patients with renal impairment
Ritonavir	600 mg SD	N/A	Moderate RI: 1.41 Severe RI: 2.11	N/A	Ritonavir pharmacokinetics have not been studied in patients with renal impairment, however, since renal clearance is negligible, a decrease in total body clearance is not expected in patients with renal impairment
Ruxolitinib	25 mg SD	Mild: 1.1 (0.9-1.36) Moderate: 1.22 (0.99-1.5) Severe: 1.03 (0.84-1.27)	Moderate RI: 1.6 Severe RI: 1.5	Mild: 1.11 (0.89-1.4) Moderate: 1.16 (0.92-1.46) Severe: 0.79 (0.63-0.99)	While there was no change in ruxolitinib PK with varying degrees of renal impairment, the PD showed increasing pharmacological activity with increased severity of renal impairment Analysis of the metabolite exposures revealed that active metabolites contributed to the observed incremental increase in PD activity Reduced dose is recommended

(Continues)

TABLE 5 (Continued)

Drug	Drug dose/regimen in the study	Average observed ratio of change in AUC	Average predicted ratio of change in AUC	Observed ratio change in C <sub>max</sub>	FDA dosage recommendation
Remdesivir	Day 1: SD 200 mg IV Days 2-10: 100 mg/day	N/A	N/A	N/A	70 The pharmacokinetics of remdesivir have not been evaluated in patients with renal impairment All patients must have an eGFR determined before dosing
Dexamethasone	8 mg SD	N/A	Moderate RI: 1.33 Severe RI: 1.31	N/A	83 The effect of baseline RI on the pharmacokinetics of dexamethasone has not been clinically studied

Abbreviations: AUC, area under concentration-time curve; BID, twice daily; C<sub>max</sub>, maximum plasma concentration; e-GFR, estimated glomerular filtration rate; ESRD, end-stage renal disease; HIV-1, human immunodeficiency virus type 1; MDRD, modification of diet in renal disease equation; N/A, no data available; PD, pharmacodynamic; PK, pharmacokinetic; Pop-PK, population pharmacokinetic; RI, renal impairment; SD, single dose; T2DM, type 2 diabetes mellitus.

is consistent with the observed effectiveness of acalabrutinib in COVID-19 patients (NCT04346199).

It has been proposed that the virus is internalized by receptor-mediated endocytosis and delivered to lysosomes, where it replicates. Some of these drugs have shown efficacy in raising the lysosomal pH (lysosomotropic drugs), resulting in lysosomal trapping of the virus and preventing its spread within the cell. This in theory might help the drug to be concentrated at the target site and thus lower doses of the drug could be required to achieve therapeutic efficacy. The lysosomotropic potentials for COVID-19 drugs were predicted based on Ufuk et al<sup>90</sup> and are shown in **Supporting Information Table S2**. The lysosomotropic potentials of chloroquine, hydroxychloroquine, atazanavir and remdesivir appeared to be beneficial for attaining a required target exposure and efficacy. However, increased exposure might also have consequences for side effects.

### 3.7 | Sensitivity analyses with varying degrees of CYP suppression by cytokine storm

The relative change in exposure (AUC) for CYP3A substrates such as acalabrutinib and ibrutinib when CYP3A expression was reduced to one-tenth of its healthy level in both the gut and liver is shown in Figure 5. As a worst-case scenario, reducing 90% of CYP3A4 abundance in the liver and gut resulted in a ~4-fold increase in AUC for acalabrutinib and dexamethasone, while a 15-fold change was found for ibrutinib. The relative change in AUC for darunavir alone was up to a 5-fold increase with reducing CYP3A4 by 90%. However, in the presence of ritonavir, this change was nearly abolished with a maximum difference in AUC of less than 4%.

## 4 | DISCUSSION

Whilst efforts to develop vaccines against COVID-19 are ongoing, there are no indications that any of the programs will provide a safe and effective vaccine at the scale needed to reverse the pandemic caused by the virus before the end of 2020. The success of public health measures in reducing the rate of infection has varied in different countries. However, as these measures ease off to balance the negative economic prospects of lockdowns and social distancing, many expect that spread of the virus will continue, albeit at lower rate, even if we managed to avoid a second peak. Therefore, effective therapeutic management of COVID cases is an essential element of the fight against the pandemic, alongside the development of vaccines and public health measures to control the spread.

There have been great advances in the use of modelling tools to predict and optimize doses and dosing schedules for clinical trials and to inform drug labels.<sup>21,91-93</sup> The current situation surrounding COVID-19 requires fast decision making in clinical trial design with limited information, resulting in potentially higher risk or reduced benefit to patients. A few such examples include higher incidence of side effects for chloroquine therapy and lack of benefit from lopinavir and



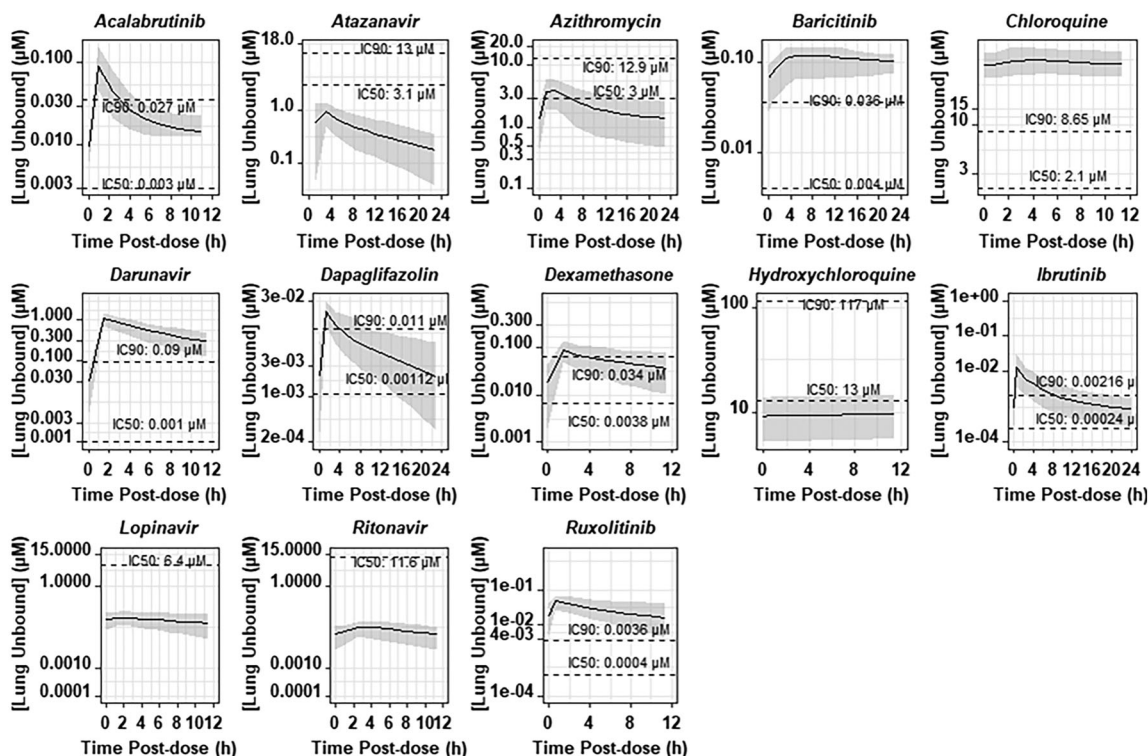
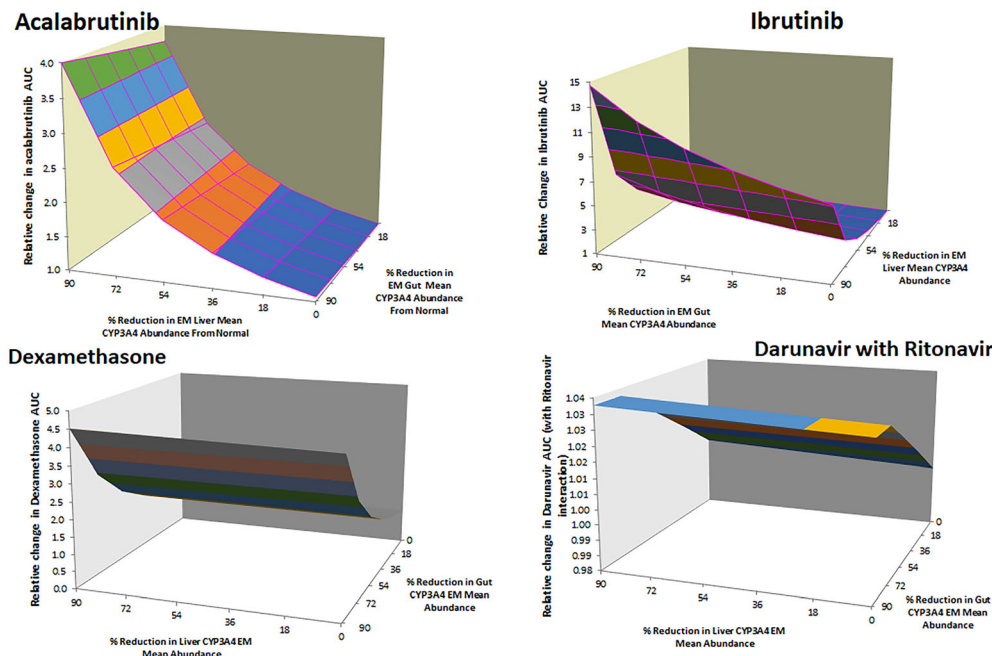


**FIGURE 4** PBPK model-based simulations of unbound drug concentration-profiles in lung tissue using a multiple-compartmental lung model in geriatric patients after verification of models using adult data for drugs that are being tested in COVID-19 trials. Dashed lines represent a relevant potency value for either IC<sub>50</sub> or IC<sub>90</sub>. Doses used for simulating lung exposure: multiple doses 14 days of dosing to steady-state azithromycin 500 mg single dose, atazanavir 400 mg, hydroxychloroquine base 155 mg, baricitinib 4 mg, chloroquine 300 mg, dapagliflozin 10 mg, acalabrutinib 100 mg, ruxolitinib 25 mg, ritonavir 600 mg, lopinavir 400 mg, darunavir 800 mg, dexamethasone 8 mg

**FIGURE 5** Sensitivity analysis on the possible effect of cytokines and consequent CYP3A4 abundance suppression in both liver and the gut on acalabrutinib (A) and ibrutinib (B) exposures



ritonavir combination therapy.<sup>94,95</sup> COVID patients who received chloroquine with azithromycin experienced QTc prolongation, which may be attributed to PK or PD changes in target tissues as a result of

DDIs. To help drug developers and regulators surrounding the development of candidate treatments and regimens for COVID-19, reliable and effective modelling tools for quantifying and comparing therapy

options, particularly in cases where clinical data are scant, will be valuable.

Typically in drug development, the effect of all extrinsic and intrinsic patient factors can be tested clinically. However, ethical and practical issues limit the numbers of studies one can feasibly conduct. As shown in **Supporting Information Figure S1**, there are more than 100 untested clinical scenarios for drugs repurposed for COVID-19 due to limited time and resources. In this current COVID-19 pandemic, PKPD and PBPK modelling tools are already helping to optimize and accelerate the use of candidate therapeutics.<sup>59,94</sup>

PBPK modelling approaches integrate drug data and physiological or system data together with patient factors to predict certain untested situations using existing knowledge. In recent years there have been several examples where PBPK modelling has been used in lieu of many clinical studies.<sup>92</sup> Currently, there is a lack of knowledge regarding the impact of intrinsic and extrinsic factors on the disposition of drugs repurposed for COVID-19. Therefore, in this work, we present a summary of ADME, PK/PD and DDI, provide a repository of PBPK models and input parameters to simulate the unbound plasma and/or lung ELF concentrations, and utilize PBPK models to predict expected alterations in drug exposure in subpopulations of COVID-19 patients which have not yet been studied, eg, in patients with older age, different race groups and hepatic/renal impairment. The drugs selected for this analysis relied on verified PBPK model availability, and robust *in vitro* and clinical evidence of their effects on drug clearance.

In many instances no clinical DDI data are available, as exemplified by the combination of ritonavir (a CYP3A reversible and time-dependent inhibitor) with BTK inhibitors such as ibrutinib and acalabrutinib. Based on PBPK modelling, the DDI risk appears to be higher with ibrutinib when combined with ritonavir (AUC ratio of ~44-fold), while ritonavir combination increased acalabrutinib AUC by 5.7-fold; however, no DDI risk is anticipated for dapagliflozin as it is mainly eliminated by UGT1A9 substrate.

As many of the repurposed drugs studied in this paper are primarily metabolized in the liver, it was unsurprising to find that impaired liver function or liver disease impacts the PK of these drugs. Baricitinib is mainly excreted unchanged by the kidney and thus its PK can be altered in renal failure conditions. PBPK models suggest dosing adjustments for CYP3A4 substrates like ibrutinib, dexamethasone and acalabrutinib are likely to be necessary.

The challenge of dosing optimization with limited time and clinical information can only be addressed as more data becomes available. We can, however, prioritize available resources to reduce the number of patients-at-risk due to suboptimal dosing and dosing schedules by simulating the situations where there is a lack of clinical data. In this way, we can establish a scientific fact-based and triaging process to further our understanding of therapeutic interventions for COVID-19. To facilitate knowledge-sharing and advance the field, modelling workspaces can be uploaded to an open-access, modelling tool platform members' area or Github (<http://github.com/>).

COVID-19 inflammatory response seems to be comparable with other chronic diseases such as cirrhosis, Rheumatoid arthritis (RA) and cancer (Table 1). Similar to these conditions, the severity and duration of COVID-19 disease is thought to impact cytokine levels and consequently metabolizing enzyme suppression, however the quantitative relationship is not yet confirmed clinically.<sup>96</sup> Due to the lack of a clear concentration-response relationship between different cytokines and the expression of drug metabolizing enzymes *in vivo*, we used sensitivity analysis to infer the potential impact of such suppression. Sensitivity analysis can be a useful tool to study the uncertainty in model input parameters and assess its impact on simulated PK profiles. For instance, in rheumatoid arthritis and cancer, it was reported that CYP3A4 content in the liver and gut was reduced by 30%<sup>20</sup> but such meta-analyses and reports are not yet available for COVID-19. Automated sensitivity analysis using different CYP3A4 substrates, including ibrutinib, dexamethasone, darunavir and acalabrutinib, suggest there is around a 4- to 15-fold increase in AUC if the CYP3A4 levels are reduced by 90% from normal levels, respectively. This indicates that exposure to these compounds will be significantly higher and more variable with varying severities of COVID-19 cytokine storm. For darunavir and ritonavir combination therapy, the change in darunavir exposure was relatively low compared to monotherapy as CYP3A4 is already inhibited by ritonavir and the impact of cytokine suppression on the enzyme is expected to be relatively low. It should be noted that dexamethasone is an anti-inflammatory drug that can reverse or mask the suppressive effect of cytokines on the expression of metabolizing enzymes. This adds to the complexity of the biological system and requires further clinical studies, not only for COVID-19 patients but also for other inflammatory diseases such as cirrhosis.

PBPK ensures more appropriate use of tissue site concentrations compared to population-based PK modelling and allows us to account for disease-drug interactions, ie, cytokine storm. In this study, we utilized *in vitro* IC<sub>50</sub> rather than *in vivo* EC<sub>50</sub> due to the scarcity of this data. Nevertheless, when unbound *in vivo* EC<sub>50</sub> data become available, one can easily update the exposure profiles with the relevant target inhibition values and explore *In vitro in vivo* extrapolation, as shown in Pilla Reddy et al.<sup>97</sup> *in vitro* IC<sub>50</sub> values were generated for antiviral drugs using serum-free media in most instances, and thus we can assume *in vitro* IC<sub>50</sub> are basically unbound values; however, *in vivo* lung tissue and plasma profiles should be corrected for lung tissue protein binding and plasma protein binding, respectively, to obtain  $K_{p,uu}$ , under the assumption that the unbound drug is pharmacologically active.<sup>59</sup>

Simulating the plasma and/or lung exposure of drugs used to treat COVID-19 is important, as the unbound tissue concentration drives the efficacy and safety of a drug. Noninvasive imaging methods (positron emission tomography/ magnetic resonance imaging) can be used to determine tissue drug concentrations; however, it is logistically challenging to routinely employ these methods during drug development. We therefore need high-throughput and cost-efficient methods to predict the tissue concentration of drugs. To achieve this, we must accurately predict drug distribution and clearance into and

out of tissue. We hypothesize that lung concentrations of drugs can be predicted through in vitro to in vivo extrapolation by incorporating the appropriate parameters such as permeability and transporter data. Preclinical, quantitative, whole-body autoradiography distribution data could be used to understand the partition between plasma and lung tissue or organ of interest to some extent, assuming the unbound partition coefficient is independent of species. Quantitative whole-body autoradiography data in rats is available for most of the drugs, facilitating comparisons with predicted total  $K_p$  values within the Simcyp simulator.

The prediction of ELF unbound concentration is particularly relevant for COVID-19 patients, as the distribution of COVID-19 drugs should be targeted into immune-privileged sites like ELF in the lung, which may represent a persistent reservoir for the virus.<sup>11</sup> Highly ionizable drugs might experience different lung uptake due to changes in lung pH resulting from COVID-19; this was accounted for in our PBPK model. One limitation of this work is that ELF concentrations were simulated using geriatric populations with reduced CYP expression in the liver and gut by 30%, which was optimized based on cancer patients.<sup>20</sup> The PK differences between healthy volunteers vs COVID-19 patients for a given drug yet to be established.

In summary, in this study we provide a database for relevant PK, PD, DDI and AE attributes for ongoing COVID-19 treatment under the investigation, including both small molecules and large molecules. Furthermore, we have demonstrated the application of quantitative modelling tools in understanding the intrinsic and extrinsic factors that can affect the PK of repurposed small molecule drugs, including the strategy of simulating plasma and/or ELF concentrations under physiological changes caused by COVID-19. Prospective PBPK modelling and simulations can identify gaps in existing datasets and help us to tackle critical clinical questions relating to patient intrinsic and extrinsic factors that cannot be studied under the time constraints of a COVID-19 pandemic.

## ACKNOWLEDGEMENTS

The authors would like to thank the patients, their families and the clinical teams who worked on the studies. E.E. is supported by PhD funding from the Egyptian government and CAPKR. V.P.R., H.J., N.G., E.L., S.S. and W.T. are all salaried employees of AstraZeneca at the time of this work.

## COMPETING INTERESTS

V.P.R., H.J., N.G., E.L., S.S. and W.T. are all employed by AstraZeneca at the time of this work. E.E. is a PhD student at University of Manchester. A.R.-H. and M.J. are employed by Certara, a company focusing on model-informed drug development.

## CONTRIBUTORS

All authors were involved in designing the studies and performing the study analyses. All authors wrote the manuscript. V.P.R., E.E. and H.J. performed the modelling analyses. All authors have approved the manuscript for submission.

## DATA ACCESSIBILITY STATEMENT

The authors confirm that the clinical data supporting the PBPK modelling are listed in [clinicaltrials.gov](https://clinicaltrials.gov) and details of these clinical studies are published elsewhere. The data that support the findings of this study are available from the Supporting Information files and the repository of PBPK files can be found in the Simcyp members area.

## ORCID

Venkatesh Pilla Reddy  <https://orcid.org/0000-0002-7786-4371>

Eman El-Khateeb  <https://orcid.org/0000-0002-8365-6528>

## REFERENCES

1. FDA. Enhancing the diversity of clinical trial populations – eligibility criteria, enrollment practices, and trial designs guidance for industry. 2019. <https://www.fda.gov/media/127712/download>, accessed 10 October 2020.
2. Beigel JH, Tomashek KM, Dodd LE, et al. Remdesivir for the treatment of Covid-19 - preliminary report. *N Engl J Med.* 2020;383:992-993.
3. Roschewski M, Lionakis MS, Sharman JP, et al. Inhibition of Bruton tyrosine kinase in patients with severe COVID-19. *Sci Immunol.* 2020; 5(48):eabd0110.
4. Treon SP, Castillo JJ, Skarbnik AP, et al. The BTK inhibitor ibrutinib may protect against pulmonary injury in COVID-19-infected patients. *Blood.* 2020;135(21):1912-1915.
5. Administration FFD. FDA guidance on conduct of clinical trials of medical products during COVID-19 public health emergency. 2020. <https://www.fda.gov/media/136238/download>, accessed 10 October 2020.
6. Jarvis CI, Van Zandvoort K, Gimma A, et al. Quantifying the impact of physical distance measures on the transmission of COVID-19 in the UK. *BMC Med.* 2020;18:1-10.
7. Gautret P, Lagier JC, Parola P, et al. Hydroxychloroquine and azithromycin as a treatment of COVID-19: results of an open-label non-randomized clinical trial. *Int J Antimicrob Agents.* 2020;56(1):105949.
8. Aziz M, Fatima R, Assaly R. Elevated Interleukin-6 and severe COVID-19: a meta-analysis. *J Med Virol.* 2020;92(11):2283-2285.
9. Shimabukuro-Vornhagen A, Gödel P, Subklewe M, et al. Cytokine release syndrome. *J Immunother Cancer.* 2018;6:56.
10. Singhal T. A review of coronavirus Disease-2019 (COVID-19). *Indian J Pediatr.* 2020;87(4):281-286.
11. Ye Q, Wang B, Mao J. The pathogenesis and treatment of the 'cytokine storm' in COVID-19. *J Infect.* 2020;80(6):607-613.
12. Morgan ET. Impact of infectious and inflammatory disease on cytochrome P450-mediated drug metabolism and pharmacokinetics. *Clin Pharmacol Ther.* 2009;85(4):434-438.
13. Williams SJ, Baird-Lambert JA, Farrell GC. Inhibition of theophylline metabolism by interferon. *Lancet.* 1987;2(8565):939-941.
14. Schmitt C, Kuhn B, Zhang X, Kivitz AJ, Grange S. Disease-drug-drug interaction involving tocilizumab and simvastatin in patients with rheumatoid arthritis. *Clin Pharmacol Ther.* 2011;89(5):735-740.
15. Lee EB, Daskalakis N, Xu C, et al. Disease-drug interaction of Sarilumab and simvastatin in patients with rheumatoid arthritis. *Clin Pharmacokinet.* 2017;56(6):607-615.
16. Keller R, Klein M, Thomas M, et al. Coordinating role of RXRalpha in downregulating hepatic detoxification during inflammation revealed by fuzzy-logic modeling. *PLoS Comput Biol.* 2016;12:e1004431.
17. Coutant DE, Kulanthaivel P, Turner PK, et al. Understanding disease-drug interactions in cancer patients: implications for dosing within the therapeutic window. *Clin Pharmacol Ther.* 2015;98(1):76-86.

18. Goralski KB, Ladda MA, McNeil JO. Drug-Cytokine Interactions. In: Pai M, Kiser J, Gubbins P, Rodvold K, eds. *Drug Interactions in Infectious Diseases: Mechanisms and Models of Drug Interactions*. Infectious Disease. Cham: Humana Press; 2018.
19. Chinnadurai R, Ogedengbe O, Agarwal P, et al. Older age and frailty are the chief predictors of mortality in COVID-19 patients admitted to an acute medical unit in a secondary care setting- a cohort study. *BMC Geriatr*. 2020;20(1):1-11.
20. Schwenger E, Reddy VP, Moorthy G, et al. Harnessing meta-analysis to refine an oncology patient population for physiology-based pharmacokinetic modeling of drugs. *Clin Pharmacol Ther*. 2018;103(2):271-280.
21. Pilla Reddy V, Bui K, Scarfe G, Zhou D, Learoyd M. Physiologically based pharmacokinetic modeling for Olaparib dosing recommendations: bridging formulations, drug interactions, and patient populations. *Clin Pharmacol Ther*. 2019;105(1):229-241.
22. Gaohua L, Wedagedera J, Small BG, et al. Development of a multicompartment permeability-limited lung PBPK model and its application in predicting pulmonary pharmacokinetics of antituberculosis drugs. *CPT Pharmacometrics Syst Pharmacol*. 2015;4(10):605-613.
23. (ASHP) ASoH-SP. Assessment of evidence for COVID-19-related treatments. <https://www.ashp.org/-/media/assets/pharmacy-practice/resource-centers/Coronavirus/docs/ASHP-COVID-19-Evidence-Table>; accessed 10 June 2020.
24. Dickmann LJ, Patel SK, Rock DA, Wienkers LC, Slatter JG. Effects of interleukin-6 (IL-6) and an anti-IL-6 monoclonal antibody on drug-metabolizing enzymes in human hepatocyte culture. *Drug Metab Dispos*. 2011;39(8):1415-1422.
25. Prystupa A, Kicinski P, Sak J, Boguszewska-Czubara A, Torun-Jurkowska A, Zaluska W. Proinflammatory cytokines (IL-1 $\alpha$ , IL-6) and hepatocyte growth factor in patients with alcoholic liver cirrhosis. *Gastroenterol Res Pract*. 2015;2015:532615.
26. Chung S. The correlation between increased serum concentrations of Interleukin-6 family cytokines and disease activity in rheumatoid arthritis patients. *Yonsei Med J*. 2011;52(1):113-120.
27. Lippitz BE, Harris RA. Cytokine patterns in cancer patients: a review of the correlation between interleukin 6 and prognosis. *Onco Targets Ther*. 2016;5:e1093722.
28. Innovative & Quality (IQ). Industry perspectives on approaches to evaluate the effect of renal impairment on drug exposure. PBSS conference, 2019 San Francisco.
29. Rowland Yeo K, Zhang M, Pan X, et al. Impact of disease on plasma and lung exposure of chloroquine, hydroxy-chloroquine and azithromycin: application of PBPK modelling. *Clin Pharmacol Ther*. 2020;108(5):976-984. <https://doi.org/10.1002/cpt.1955>
30. Retallack H, Di Lullo E, Arias C, et al. Zika virus cell tropism in the developing human brain and inhibition by azithromycin. *Proc Natl Acad Sci USA*. 2016;113(50):14408-14413.
31. Gielen V, Johnston SL, Edwards MR. Azithromycin induces anti-viral responses in bronchial epithelial cells. *Eur Respir J*. 2010;36(3):646-654.
32. Bacharier LB, Guilbert TW, Mauger DT, et al. Early administration of azithromycin and prevention of severe lower respiratory tract illnesses in preschool children with a history of such illnesses: a randomized clinical trial. *JAMA*. 2015;314(19):2034-2044.
33. USA G. HIGHLIGHTS OF PRESCRIBING INFORMATION: XOFLUZATM (baloxavir marboxil) tablets, for oral use. In: FDA US Food & Drug Administration, October 2019.
34. Warhurst DC, Steele JCP, Adagu IS, Craig JC, Cullander C. Hydroxychloroquine is much less active than chloroquine against chloroquine-resistant Plasmodium falciparum, in agreement with its physicochemical properties. *J Antimicrob Chemother*. 2003;52(2):188-193. <https://doi.org/10.1093/jac/dkg319>
35. Yao X, Ye F, Zhang M, et al. In vitro antiviral activity and projection of optimized dosing Design of Hydroxychloroquine for the treatment of severe acute respiratory syndrome coronavirus 2 (SARS-CoV-2). *Clin Infect Dis*. 2020;71(15):732-739.
36. Liu J, Cao R, Xu M, et al. Hydroxychloroquine, a less toxic derivative of chloroquine, is effective in inhibiting SARS-CoV-2 infection in vitro. *Cell Discov*. 2020;6(1):1-4.
37. Han S, Hagan DL, Taylor JR, et al. Dapagliflozin, a selective SGLT2 inhibitor, improves glucose homeostasis in normal and diabetic rats. *Diabetes*. 2008;57(6):1723-1729.
38. Lv Z, Chu Y, Wang Y. HIV protease inhibitors: a review of molecular selectivity and toxicity. *HIV AIDS (Auckl)*. 2015;7:95-104.
39. Fintelman-Rodrigues N, Sacramento CQ, Lima CR, et al. Atazanavir, alone or in combination with ritonavir, inhibits SARS-CoV-2 replication and proinflammatory cytokine production. *Antimicrob Agents Chemother*. 2020;64(10):e00825-20.
40. Richardson P, Griffin I, Tucker C, et al. Baricitinib as potential treatment for 2019-nCoV acute respiratory disease. *Lancet (London, England)*. 2020;395:e30.
41. Roskoski R Jr. Janus kinase (JAK) inhibitors in the treatment of inflammatory and neoplastic diseases. *Pharmacol Res*. 2016;111:784-803.
42. Warren TK, Jordan R, Lo MK, et al. Therapeutic efficacy of the small molecule GS-5734 against Ebola virus in rhesus monkeys. *Nature*. 2016;531(7594):381-385.
43. McMullan LK, Flint M, Chakrabarti A, et al. Characterisation of infectious Ebola virus from the ongoing outbreak to guide response activities in the Democratic Republic of the Congo: a phylogenetic and in vitro analysis. *Lancet Infect Dis*. 2019;19(9):1023-1032.
44. Siegel D, Hui HC, Doerffler E, et al. Discovery and synthesis of a phosphoramidate prodrug of a pyrrolo[2,1-f][triazin-4-amino] adenine C-nucleoside (GS-5734) for the treatment of Ebola and emerging viruses. *J Med Chem*. 2017;60(5):1648-1661.
45. Yu R, Song D, DuBois DC, Almon RR, Jusko WJ. Modeling combined anti-inflammatory effects of dexamethasone and Tofacitinib in arthritic rats. *AAPS J*. 2019;21:93-101.
46. Loew D, Schuster O, Graul EH. Dose-dependent pharmacokinetics of dexamethasone. *Eur J Clin Pharmacol*. 1986;30(2):225-230.
47. Tocilizumab FDA label. <Tocilizumab FDA label.pdf>.
48. Abdallah H, Hsu JC, Lu P, et al. Pharmacokinetic and pharmacodynamic analysis of subcutaneous Tocilizumab in patients with rheumatoid arthritis from 2 randomized, controlled trials: SUMMACTA and BREVACTA. *J Clin Pharmacol*. 2017;57(4):459-468.
49. Mihara M, Ohsugi Y, Kishimoto T. Tocilizumab, a humanized anti-interleukin-6 receptor antibody, for treatment of rheumatoid arthritis. *Open Access Rheumatol*. 2011;3:19-29.
50. Amgen. Product monograph: Kineret® (anakinra) [online] Available from URL: <http://www.kineretrx.com> [Accessed 2020 Aug 24].
51. Hensley LE, Fritz LE, Jahrling PB, Karp CL, Huggins JW, Geisbert TW. Interferon-beta 1a and SARS coronavirus replication. *Emerg Infect Dis*. 2004;10:317-319.
52. Anakinra BLA. [https://www.accessdata.fda.gov/drugsatfda\\_docs/nda/2001/103950-0\\_Kineret\\_Biopharmr.PDF](https://www.accessdata.fda.gov/drugsatfda_docs/nda/2001/103950-0_Kineret_Biopharmr.PDF). 2001.
53. Siltuximab BLA. [https://www.accessdata.fda.gov/drugsatfda\\_docs/nda/2014/125496Orig1s000MedR.pdf](https://www.accessdata.fda.gov/drugsatfda_docs/nda/2014/125496Orig1s000MedR.pdf)
54. Alexander SPH, Fabbro D, Kelly E, et al. The Concise Guide to PHARMACOLOGY 2019/20: Enzymes. *Brit J Pharmacol*. 2019;176:S297-S396. <https://doi.org/10.1111/bph.14752>
55. Roytblat L, Rachinsky M, Fisher A, et al. Raised interleukin-6 levels in obese patients. *Obes Res*. 2000;8(9):673-675.
56. Hidaka T, Suzuki K, Kawakami M, et al. Dynamic changes in cytokine levels in serum and synovial fluid following filtration leukocytapheresis therapy in patients with rheumatoid arthritis. *J Clin Apher*. 2001;16(2):74-81.
57. Arican O, Aral M, Sasmaz S, Ciragil P. Serum levels of TNF-alpha, IFN-gamma, IL-6, IL-8, IL-12, IL-17, and IL-18 in patients with active psoriasis and correlation with disease severity. *Mediators Inflamm*. 2005;2005(5):273-279.

58. Ataseven H, Bahcecioglu IH, Kuzu N, et al. The levels of ghrelin, leptin, TNF-alpha, and IL-6 in liver cirrhosis and hepatocellular carcinoma due to HBV and HDV infection. *Mediators Inflamm.* 2006;2006:78380.
59. Fan J, Zhang X, Liu J, et al. Connecting hydroxychloroquine in vitro antiviral activity to in vivo concentration for prediction of antiviral effect: a critical step in treating COVID-19 patients. *Clin Infect Dis.* 2020.
60. Acalabrutinib FDA NDA. Highlights of prescribing information for Calquence (acalabrutinib) capsules, for oral use. 2017.
61. Azithromycin FDANDA. Highlights of prescribing information for Zithromax (azithromycin) for IV infusion only. 2017.
62. Baricitinib FDA NDA. Highlights of prescribing information: Olumiant (baricitinib) tablets, for oral use. 2018.
63. Baloxavir FDA NDA. Highlights of prescribing information: Xofluza (baloxavir marboxil). 2018.
64. Chloroquine FDA NDA. ARALEN chloroquine phosphate, USP label. 2018.
65. Hydroxychloroquine FDA NDA. PLAQUENIL Hydroxychloroquine sulfate tablets, USP. 2019.
66. Darunavir, FDA NDA, Darunavir. [https://www.accessdata.fda.gov/drugsatfda\\_docs/label/2017/021976s045\\_202895s020lbl.pdf](https://www.accessdata.fda.gov/drugsatfda_docs/label/2017/021976s045_202895s020lbl.pdf). 2017.
67. Dapagliflozin FDA NDA, FDA. Highlights of prescribing information for FARXIGA (dapagliflozin). In, January 2020.
68. de Zwart L, Snoeys J, De Jong J, Sukbuntherng J, Mannaert E, Monshouwer M. Ibrutinib dosing strategies based on interaction potential of CYP3A4 perpetrators using physiologically based pharmacokinetic modeling. *Clin Pharmacol Ther.* 2016;100(5):548-557.
69. Ibrutinib FDA NDA. [https://www.accessdata.fda.gov/drugsatfda\\_docs/label/2018/210563s000lbl.pdf](https://www.accessdata.fda.gov/drugsatfda_docs/label/2018/210563s000lbl.pdf). 2018.
70. Remdesivir FDA Label. Fact sheet for health care providers: emergency use authorization (EUA) of Remdesivir (GS-5734). In, 2020, May 1.
71. Ruxolitinib FDA Label. Highlights of prescribing information for JAKAFI (ruxolitinib) tablets, for oral use. 2011.
72. Ritonavir FDA label. Highlights of prescribing information for NORVIR (ritonavir) tablet, for oral use/ oral solution/oral powder. 2017.
73. Acalabrutinib FDA NDA. NDA/BLA multi-disciplinary review and evaluation {NDA 210259} {CALQUENCE, acalabrutinib}. In, edResearch CfDEa, FDA US Food & Drug Administration, 2016, February 1.
74. de Jong J, Skee D, Hellemans P, et al. Single-dose pharmacokinetics of ibrutinib in subjects with varying degrees of hepatic impairment. *Leuk Lymphoma.* 2017;58(1):185-194.
75. Mazzei T, Surrenti C, Novelli A, et al. Pharmacokinetics of azithromycin in patients with impaired hepatic function. *J Antimicrob Chemother.* 1993;31(Suppl E):57-63.
76. Gustafsson LL, Walker O, Alvan G, et al. Disposition of chloroquine in man after single intravenous and oral doses. *Br J Clin Pharmacol.* 1983;15(4):471-479.
77. Tett SE, Cutler DJ, Day RO, Brown KF. Bioavailability of hydroxychloroquine tablets in healthy volunteers. *Br J Clin Pharmacol.* 1989;27(6):771-779.
78. FDA Center for Drug Evaluation and Research. Summary of Resubmission and DPARB/OND Recommendations. Baricitinib, NDA 207924. [https://www.accessdata.fda.gov/drugsatfda\\_docs/nda/2018/207924Orig1s000SumR.pdf](https://www.accessdata.fda.gov/drugsatfda_docs/nda/2018/207924Orig1s000SumR.pdf) Accessed Feb 7, 2020.
79. Peng JZ, Pulido F, Causemaker SJ, et al. Pharmacokinetics of lopinavir/ritonavir in HIV/hepatitis C virus-coinfected subjects with hepatic impairment. *J Clin Pharmacol.* 2006;46(3):265-274.
80. Bristol Myers Squibb Company. Reyataz (atazanavir sulfate) capsules: prescribing information. 2005. [https://www.accessdata.fda.gov/drugsatfda\\_docs/label/2005/021567s005lbl.pdf](https://www.accessdata.fda.gov/drugsatfda_docs/label/2005/021567s005lbl.pdf)
81. Sekar V, Spinosa-Guzman S, De Paepe E, et al. Pharmacokinetics of multiple-dose darunavir in combination with low-dose ritonavir in individuals with mild-to-moderate hepatic impairment. *Clin Pharmacol.* 2010;49(5):343-350.
82. Chen X, Shi JG, Emm T, et al. Pharmacokinetics and pharmacodynamics of orally administered ruxolitinib (INCB018424 phosphate) in renal and hepatic impairment patients. *Clin Pharmacol Drug Dev.* 2014;3(1):34-42.
83. US Food and Drug Administration. Highlights of prescribing information: Hemady (Dexamethasone). [https://www.accessdata.fda.gov/drugsatfda\\_docs/label/2019/211379s000lbl.pdf](https://www.accessdata.fda.gov/drugsatfda_docs/label/2019/211379s000lbl.pdf)
84. Hoffer D, Koeppe P, Paeske B. Pharmacokinetics of azithromycin in normal and impaired renal function. *Infection.* 1995;23(6):356-361.
85. Salako LA, Walker O, Iyun AO. Pharmacokinetics of chloroquine in renal insufficiency. *Afr J Med Med Sci.* 1984;13(3-4):177-182.
86. Kasichayanula S, Liu X, Pe Benito M, et al. The influence of kidney function on dapagliflozin exposure, metabolism and pharmacodynamics in healthy subjects and in patients with type 2 diabetes mellitus. *Br J Clin Pharmacol.* 2013;76(3):432-444.
87. US Food and Drug Administration. Highlights of prescribing information: Kaletra (Lopinavir and ritonavir). [https://www.accessdata.fda.gov/drugsatfda\\_docs/label/2016/021251s052\\_021906s046lbl.pdf](https://www.accessdata.fda.gov/drugsatfda_docs/label/2016/021251s052_021906s046lbl.pdf)
88. Jeon S, Ko M, Lee J, et al. Identification of antiviral drug candidates against SARS-CoV-2 from FDA-approved drugs. *Antimicrob Agents Chemother.* 2020;64(7):e00819-00820.
89. Hoffmann M, Mosbauer K, Hofmann-Winkler H, et al. Chloroquine does not inhibit infection of human lung cells with SARS-CoV-2. *Nature.* 2020;585(7826):588-590.
90. Ufuk A, Assmus F, Francis L, et al. In vitro and in silico tools to assess extent of cellular uptake and lysosomal sequestration of respiratory drugs in human alveolar macrophages. *Mol Pharm.* 2017;14(4):1033-1046.
91. Pilla Reddy V, Walker M, Sharma P, Ballard P, Vishwanathan K. Development, verification, and prediction of Osimertinib drug-drug interactions using PBPK modeling approach to inform drug label. *CPT Pharmacometrics Syst Pharmacol.* 2018;7(5):321-330.
92. Shebley M, Sandhu P, Emami Riedmaier A, et al. Physiologically based pharmacokinetic model qualification and reporting procedures for regulatory submissions: a consortium perspective. *Clin Pharmacol Ther.* 2018;104(1):88-110.
93. Taskar KS, Pilla Reddy V, Burt H, et al. Physiologically-based pharmacokinetic models for evaluating membrane transporter mediated drug-drug interactions: current capabilities, case studies, future opportunities, and recommendations. *Clin Pharmacol Ther.* 2020;107(5):1082-1115.
94. Verscheijden LFM, van der Zanden TM, van Bussel LPM, et al. Chloroquine dosing recommendations for pediatric COVID-19 supported by modeling and simulation. *Clin Pharmacol Ther.* 2020;108(2):248-252.
95. Cao B, Wang Y, Wen D, et al. A trial of Lopinavir-ritonavir in adults hospitalized with severe Covid-19. *N Engl J Med.* 2020;382(19):1787-1799.
96. Azam YJ, Machavaram KK, Rostami-Hodjegan A. The modulating effects of endogenous substances on drug metabolising enzymes and implications for inter-individual variability and quantitative prediction. *Curr Drug Metab.* 2014;15(6):599-619.
97. Pilla Reddy V, Anjum R, Grondine M, et al. The pharmacokinetic-pharmacodynamic (PKPD) relationships of AZD3229, a novel and selective inhibitor of cKIT, in a range of mouse xenograft models of GIST. *Clin Cancer Res.* 2020;26(14):3751-3759.

## SUPPORTING INFORMATION

Additional supporting information may be found online in the Supporting Information section at the end of this article.

**How to cite this article:** Pilla Reddy V, El-Khateeb E, Jo H, et al. Pharmacokinetics under the COVID-19 storm. *Br J Clin Pharmacol.* 2021;1-29. <https://doi.org/10.1111/bcp.14668>